HOCHSCHULE FRESENIUS
UNIVERSITY OF APPLIED SCIENCES

Chemistry & Biology

Master of Bio- and Pharmaceutical Analysis

Idstein

Synthesis of modifications of an adenylyl cyclase inhibitor conjugated with a peptide and folic acid for the application in tumor immunotherapy

Approved MASTER THESIS

for the achievement of an academic degree as

Master of Science

Lisa-Maria Ackermann

born in Langen

1st Consultant: Prof. Dr. M. Buchholz

2nd Consultant: Mr. Sascha Klein

26. July 2013

Under closure until: 26. July 2016

This Thesis was written between 18.02.2013 and 26.07.2013 at the Max-Planck Institute for Polymer Research in the group of Professor Dr. Klaus Müllen under support and supervision of Dr. Kalina Peneva.

Contents

List of figures

List of tables

Abbreviations

AB	Antibody
AC	Adenylyl cyclase
Ac_2O	Acetic acid anhydride
AMP	Adenosine monophosphate
ATP	Adenosine triphosphate
AUC	Area under the curve
cAMP	Cyclic Adenosine monophosphate
$CDCl_3$	Deuterated chloroform
CDE	Clathrin-dependent endocytosis
CDI	Clathrin-independent endocytosis
CPP	Cell-penetrating peptide
CREB	Transciption factor
CTLA-4	Cytotoxic T-Lymphocyte Antigen 4
DCC	*N*,*N*'-Dicyclohexylcarbodiimid
DCM	Dichloromethane
DDS	Drug-delivery-system
DIC	*N*,*N*'-Diisopropylcarbodiimid
DIPEA	Diisopropylethylamine
DMAP	4-(Dimethylamino)-pyridin
DMSO	Dimethylsulfoxide
DNA	Deoxyribonucleic acid
DPBS	Dulbecco’s phosphate buffered saline

DTIC	Dacarbazine
EMA	European medicines agency
ERK	Extracellular-signal regulated kinase
ESI	Electrospray ionization time of flight mass spectrometry
EtOAc	Ethylacetate
FA	Folic acid
FA-SH	Folic acid cysteamine
FDA	Food and drug administration
GJIC	Gap junction intermolecular communication
GPCR	G-protein coupled receptor
HD IL-2	High dose Interleukin-2
HPLC	High pressure liquid chromatography
ICER	Transcriptional suppressor
IFN-α	Interferon-α
IL	Interleukin
MALDI	Matrix assisted laser desportion ionisation
MEK	Mitogen-activated protein kinase
MeOH	Methanol
MS	Mass spectrometry
NHS	N-Hydroxysuccinimide
NMR	Nuclear magnetic resonance
nTreg	Naturally occurring regulatory T-cell
PDE	Phosphodiesterase

PKA	Protein kinase A
PTD	Protein transduction domain
resT	Responding T-cell
TEA	Triethylamine
TEAA	Triethylammoniumacetate
TFA	Trifluoroacetic acid
TLC	Thin layer chromatography
ToF	Time of flight
TSTU	2-Succinimido-1,1,3,3-tetramethyluronium-tetrafluorborat

Acknowledgement

I would like to thank Professor Dr. Klaus Müllen for the opportunity to write this Master thesis in his research group at the Max-Plank Institute for Polymer Research.

Furthermore I thank my two supervisors Dr. Kalina Peneva and Prof. Dr. Monika Buchholz for their support.

Additionally I thank Dr. M. Wagner and N. Hanold for measuring NMR spectra and ESI-MS of my samples.

Für meinen Vater Peter Ackermann & voor mijn moeder Nesia Ackermann

1 Introduction

Cancer is the second most frequent cause of death after cardio-vascular-diseases in Germany [1]. Besides others, melanoma is one of the most frequent forms of cancer [2]. During this disease, which mostly affects women at an average age of 60, men at 66 [3], the patient forms black tumors on the skin [4]. The big problem occurring in the progression of the disease is not the cancer on the skin itself, but the high probability of forming metastasis [5]. Since chemotherapy being one of the common procedures to treat cancer is not effective in melanoma [6], it is crucial to find other approaches to influence the progress of the disease.

One alternative to the well-established chemotherapy is the so called immunotherapy, also referred to as biotherapy [7]. This approach deals with the modification of the immune system or the utilization of parts of the immune system as cancer treatment [7]. The general idea is the targeted treatment of cancer cells without affecting healthy cells by boosting the immune system, thus harnessing the potential of the host immune system to detect and eliminate transformed cells [8]. This can be achieved for example by the use of antibodies selectively recognizing antigen structures on the outer membrane of the tumor [9]. This principle can either be used to help the immune system detecting the cancer cells as foreign and start attacking them or harnessing the antibody as carrier for other potent anti-cancer drugs to be transported to their destination. As detailed described by Robert O. Dillman [7], several other types of immunotherapy exist. Rituximab is targeting a certain protein expressed on lymphomas, Trastuzumab is affecting a tumor antigen, just to mention two of the immunotherapy agents that made it into clinical use [8]. To conclude, the advantage of immunotherapy based treatment, compared to commonly applied chemotherapy is the targeted effect on the cancer cells and therefore avoiding the dose-limiting toxicity of chemotherapy resulting in lower side-effects and protection of healthy cells [10].

Also melanoma is medicated with immunotherapy. Ipilimumab is a monoclonal antibody conjugate which is able to interfere with the immune system, particularly blocking the regulatory T-cells (nT_{reg}) [7]. This drug is approved in Switzerland since 2011 and commercially available as Yervoy® and is also approved by the food and drug administration (FDA) in the US [9]. nT_{reg} cells have immune-suppressive properties, thus blocking those leads to a stimulation of the immune system [8]. Since the immune system misunderstands tumor cells as “self” and therefore inhibits their eradication by effector T-

cells, excitation of this component is a promising approach to force the immune system to attack the malignant cells [8]. Based on this strategy, influencing nT_{reg} cells is focused in this project. An inhibitor is applied, targeting the second messenger used by the cells to communicate and therefore control the immune-suppressive properties of nT_{reg}-cells [11].

1.1 Motivation and objectives

The aim of this work is the design and synthesis of novel adenylyl cyclase inhibitors containing a cleavable linker and targeting moiety for improving melanoma-specific T-cell responses by cAMP-mediated disarming of regulatory T-cells and therefore the attenuation of the progress of melanoma cancer.

Since commonly applied chemotherapy is often ineffective in melanoma skin cancer, the development of new alternatives is crucial. One approach is cancer immunotherapy, which modifies the immune system or utilizes parts of it, for example antibodies. Those components can be harnessed either as marker to help the immune system to recognize the cancer cells or as carrier for potent anti-cancer drugs.

In this project it is focused on a drug which is used in cancer research called NKY-80 (2-amino-7-(2-furanyl)-7,8-dihydro-5(6H)-quinazolinone). It inhibits adenylyl cyclase (AC), the enzyme converting adenosinetriphosphate (ATP) to cyclic adenosine monophosphate (cAMP), an important second messenger fulfilling several tasks. It is included in for example activating protein kinases (PKA), which are enzymes being involved in phosphorylation of different cellular proteins which subsequently regulate cell division, cell differentiation, and ion transport or ion channels. Especially cell division and cell differentiation are, besides their invasiveness and the ability to build metastasis, the key properties distinguishing cancer cells from normal cells. An intervention in these pathways thus is able to influence the progress of cancer. Furthermore, cAMP plays a central role in the suppression of the immune system. nT_{reg}-cells control the immune system and are able to suppress it in order to avoid autoimmunity, allergies and anti-tumor responses as well [12]. Since nT_{reg}-cells mediate their suppressive function by transferring cAMP into responding T-cells (resT) via gap junction intercellular communication (GJIC) and cAMP is a general inhibitor of T-cell growth, differentiation and proliferation, the intervention in its generation and dismantling can be an approach to interfere in the function of nT_{reg}-cells [13]. The connection between AC, NKY-80 and nT_{reg} is displayed in Figure 1.

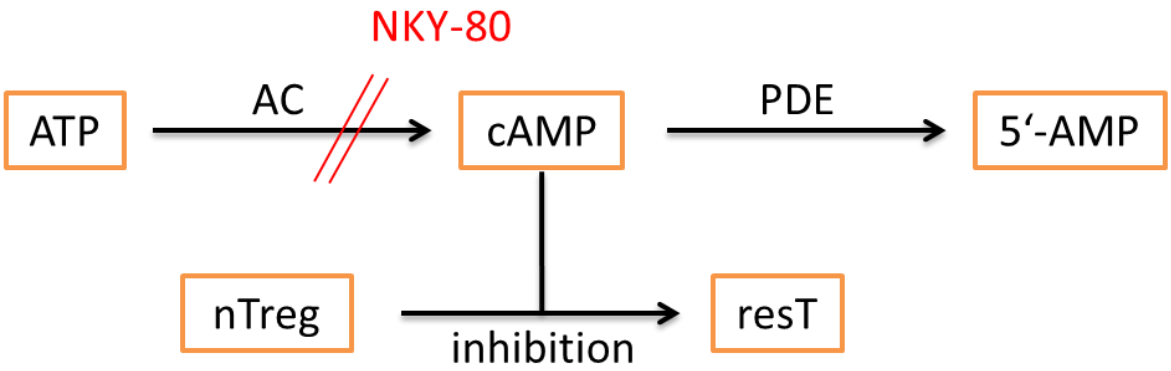

Figure 1: Generation and degradation of cAMP and its key role as second messenger in the GJIC between nTreg and resT. ATP=Adenosinetriphosphate, AC=Adenylyl cyclase, cAMP=cyclic Adenosinemonophosphate, PDE=Phosphodiesterase, nTreg=naturally occurring regulatory T-cells, resT=responding T-cells

During this project, the above mentioned drug NKY-80 should be coupled to a cell-penetrating peptide (CPP). This could be accomplished by the synthesis of a linker bearing two functionalities. These offer the possibility to link the NKY-80 via a pH sensitive hydrazone bond, and on the other side making a connection with the peptide possible via disulfide bond. The big advantage of introducing a disulfide is the variable applications this moiety can be used for as displayed in Figure 2.

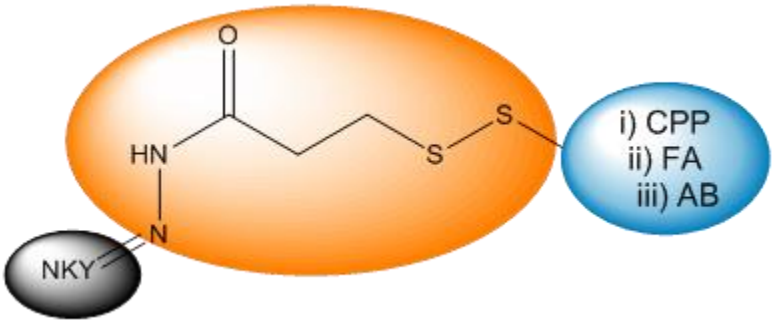

Figure 2: Structure of the linker (orange) coupled to NKY (black) via hydrazone. Additional capability to bind different carriers (blue): i) CPP=cell-penetrating peptide, ii) FA=folic acid, iii) AB=antibody by forming a disulfide bond

NKY-80 itself lacks in potency which is why it requires the coupling to a carrier, but this also needs to fulfill the targeting demand. During this project, NKY-80 should be coupled to a cell-penetrating peptide via a linker, which will also be synthesized within this project. As described, cAMP is involved in miscellaneous pathways within the body, making a

systematically administration of NKY-80 impossible. Although the coupling to a CPP should increase the uptake level of the drug into a cell, it would not improve the selectivity of the drug. But since melanoma is represented on the skin, a direct injection into the tumor could be possible, bypassing the selectivity problem. In order to also treat the metastasis occurring frequently when suffering from skin cancer, a targeting application is also necessary. This could be achieved by coupling NKY-80 via the introduced linker to either an antibody or a folic acid, since both act via receptor mediated endocytosis [14, 15]. To target nT_{reg}-cells the conjugate with antibodies (AB), for targeting melanoma cells the folic acid conjugate could be applied.

The synthesis of folic acid containing NKY-80 will be carried out during this project. Since quickly dividing cells have a higher consumption and need of folic acid for reproducing themselves, they express more folic acid receptors on their cell membrane than “normal” cells do [16]. This fact can be exploited to target these quickly dividing cells, thus cancer cells [17]. In order to attach the linker to folic acid, a thiol has to be introduced into the vitamin, which should be achieved by the conversion with 2-aminoethanethiol.

In brief, a linker bearing a hydrazine and an activated thiol will be synthesized in a two-step reaction. An adenylyl cyclase inhibitor called NKY-80 will be attached by the formation of a hydrazone bond. On the other side the thiol offers the possibility of coupling either a cell-penetrating peptide or a folic acid moiety, which will be both performed during this project. All products will be characterized using NMR spectroscopy and mass spectrometry.

2 General part

2.1 Cancer and Melanoma

2.1.1 General procedure of treating cancer

About 26 % (221.500 people) died because of cancer in Germany in 2011, thereof 119.755 men and 101.836 women. The former suffer from cancer affecting the intestinal tract (32 %) or the respiratory system (26 %). Also females die most commonly due to intestinal cancer (30 %), followed by breast cancer (18 %). Siegel et al. report that 5 % of all new diagnoses of cancer are accounted for melanoma in 2012 in the US. The mortality rate increased from 8790 in 2011 to 9180 in 2012. Due to the general permanently increasing number of cancer patients this means, that 1 of 3 women and 1 of 2 men will develop cancer during his or her lifetime in the US Thereof 7 % of both, men and women, are affected by melanoma [18-20].

Three different procedures which are mainly applied in the treatment of cancer are available, surgical excision, irradiation and drug therapy, also called chemotherapy. Depending on the type and the progress of the disease, the patient is treated in a different way with one of the above mentioned approaches or combinations of them. The big difficulty in cancer therapy is the differentiation between malignant and healthy cells.

In case of melanoma the affected skin part is excised. Depending on the progress, the size of the removed area around the mole varies. Furthermore, the closest located lymph node can also be eliminated [21].
Additionally, chemotherapy is applied to melanoma, on which patients do not respond in every case [6]. Therefore immunotherapy is a promising alternative to treat melanoma. In immunotherapy the immune system is activated to eliminate or attenuate the progress of the tumor [7, 8]. Different approaches exist, focusing on different pathways within the tumor cell.

The standard chemotherapy agent used for the treatment of melanoma is Dacarbazine (DTIC). It is the only one being approved by both, the FDA (food and drug administration) and the EMA (European medicines agency) [22]. Dacarbazine is a monofunctional triazene alkylating the bases of the DNA when administered to a cell which stops the

proliferation [23]. However, DTIC has shown objective responses for only 15.3 % and complete response rates for 4.1 %, tested with 3356 patients in more than 20 studies [24].

Besides chemotherapy, melanoma is treated with immunotherapy agents like high-dose interleukin-2 (HD IL-2) or Interferon-α (IFN-α) [25]. Drawbacks of these drugs are also the low response rates, as well as the high toxicity especially in high dose application and the associated side-effects. In order to optimize the efficiency, INF-α was pegylated and combinations of chemotherapy and immunotherapy as well as mulitdrugchemotherapy was tested in clinical trials. Approaches including IL-2 and IFN-α led to higher responses, but associated with this, toxicities also increased [25].

Vemurafenib, Ipilimumab and Tremelimumab are immunotherapy agents containing a monoclonal antibody targeting different pathways within a tumor cell in order to stop the progress. Vemurafenib strongly and selectively inhibits mutant BRAF being part of the RAS/RAF/MEK/ERK (MEK=mitogen-activated protein kinase, ERK=extracellular-signal regulated kinase) pathway. This pathway is responsible for the conversion of stimulatory signals of growth factors by binding to their cognate receptors on the outer membrane, resulting in activation of several cytoplasmic and nuclear substrates. A genetic mutation in the BRAF gene (called V600E mutation, valine to glutamic acid substitution at codon 600) which is very common in melanoma, leads to significant activation of ERK and therefore supporting cell proliferation and survival. Vemurafenib is just effective for patients suffering from $BRAF^{V600E}$ mutation, but even after successful cure, patients experience tumor recurrence or develop resistance against the drug. Consequently, multi- instead of monodrug therapy is suggested [26].

Ipilimumab and Tremelimumab target cytotoxic T-lymphocyte antigen 4 (CTLA-4), a membrane protein on T-cells where it acts as a negative regulator. The drugs are capable of increasing T-cell activity by blocking of negative regulation signals. Thus, they inhibit the CTLA-4 protein which down regulates the immune system and therefore antitumor immunity is supported. Ipilimumab bears the benefit of improving the 1-year and 2-year survival rates, which has been tested with 676 people by Hodi et al in 2010, but it also reaches low response rates when used as single therapy [27]. Tremelimumab did not lead to improved survival when compared with DTIC [28].

2.1.2 Genesis of a cancer cell

Due to mutations in the DNA, a normal cell can become a cancer cell. This can have several reasons like being inherited, acquired or as a result of exposure to carcinogen substances like tobacco or as an effect of viruses. Furthermore, the activation of proto-oncogenes (control cell division, apoptosis and differentiation) to oncogenes (induce malignant change by viral or carcinogen action) as well as the inactivation of tumor suppressor genes (anti-oncogenes) higher the potency of contracting cancer. The characteristics that distinguish cancer cells from normal cells are uncontrolled proliferation, dedifferentiation and loss of function, invasiveness and the ability to form metastasis. Besides that, a tumor consists of different types of cells which make a successful therapy difficult. About 5 % of the cells are dividing cells, which can easily be affected by chemotherapy. In addition to that there are cells which do not divide anymore but be a part of the tumor, bearing no problem because they cannot harm the body anymore. But the biggest risk comes from the resting cells, which are not dividing anymore, thus are not affected by the common therapy which affects the cell division in most cases, but do still have the possibility to start proliferation again [29].

In case of melanoma the highly malign tumor is coming from the melanocytes. It forms metastasis already in early stage in the lymph nodes and haematogenic. The quick invasion of melanoma cells into the thin lymph tissue or upper dermis and therefore early metastasis is explained by the fact that benign and malign melanocytes do not grow in cell groups and do not form intracellular bridges [21]. The genesis includes several steps which can undergo a linear or non-linear sequence [5]. The detailed correlation is explained by Villanueva et al. [30].

2.2 Signal transduction to influence the regulatory T-cells

cAMP is an important second messenger bearing miscellaneous functions. It is generated from adenosinetriphosphate (ATP) by adenylyl cyclase (AC) and degraded to 5'-adenosinemonophosphate (5'-AMP) by phosphodiesterase (PDE).

Mammals express ten different isoforms of AC, which are membranous bound enzymes being activated by binding of hormones and neurotransmitters to their G-Protein-coupled receptors (GPCR) [31]. The catalytic core of AC is made up by two cytosolic, pseudosymmetrically domains (C1 and C2) with six predicted helices each. At their interface they form the catalytic site and the regulatory diterpene site. The different

isoforms are differentially expressed in different cells and tissues, leading to the assumption they having specific (patho)physiological functions [32]. The stimulation and influence of AC is displayed in Figure 3.

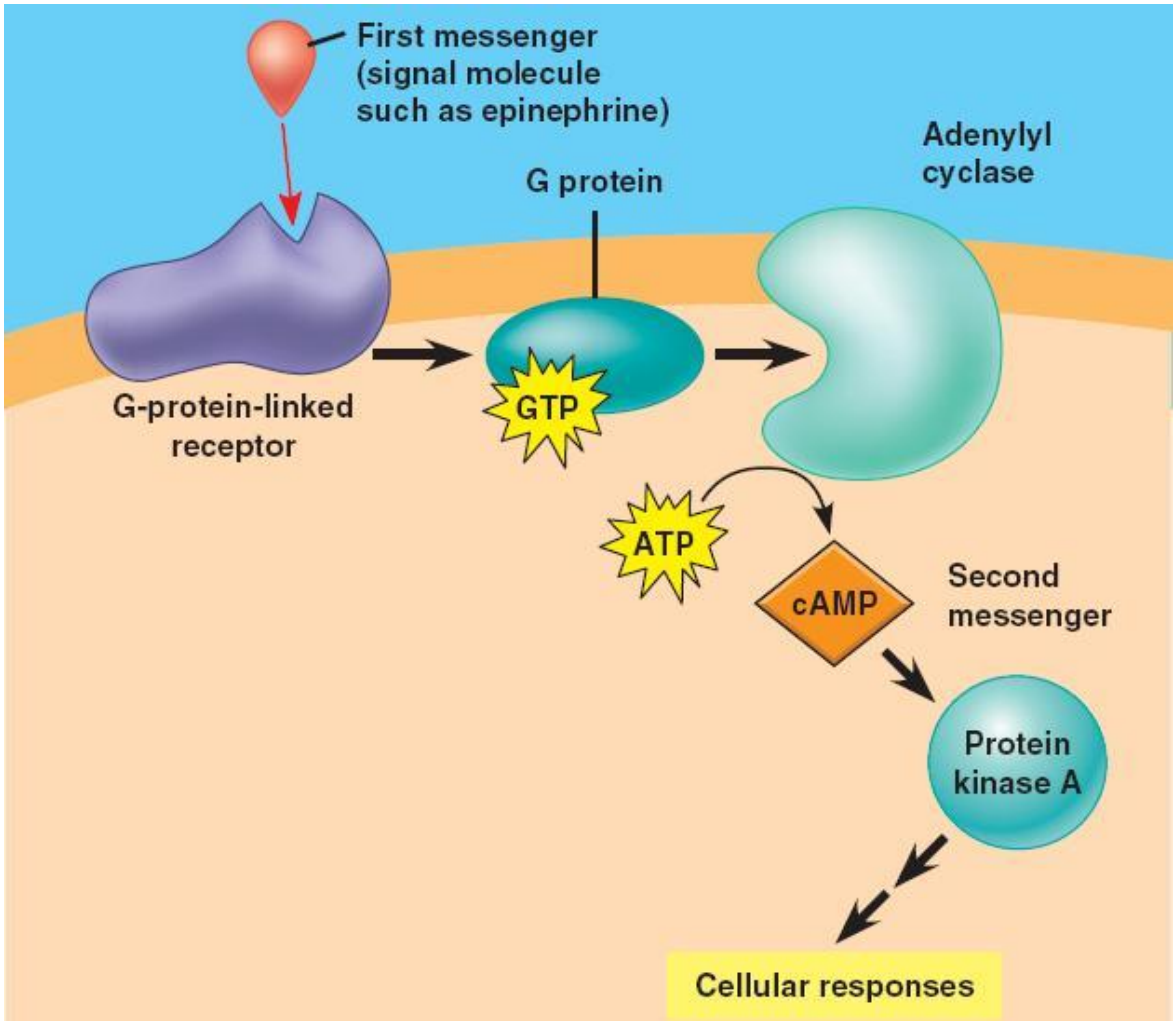

Figure 3: Signal transduction pathway of adenylyl cyclase [33]. GTP=Guanosinetriphosphate, ATP=Adenosinetriphosphate, cAMP=cyclic Adenosinemonophosphate

In general ACs catalyze the generation of cAMP, which activates the protein kinase A (PKA). This in turn controls the function of several cellular proteins by regulating protein phosphorylation. Furthermore, enzymes involved in energy metabolism, cell division, cell differentiation, ion transport and channels and contractile proteins in smooth muscle are influenced and modulated by PKA [29]. Besides this, cAMP is crucial for the maintenance of the immune system. nT_{reg}-cells are a thymus derived subset of T-cells which are of capital importance for preventing autoimmunity [8]. They transfer cAMP via gap junction intermolecular communication (GJIC) to resT, resulting in inhibition of IL-2 gene

expression [12], which means that the immune response is decreased, since IL-2 is essential for proliferation and differentiation of T-cells [34]. The exact underlying molecular mechanism still remains unclear, but Bodor et al. [35] suggest, that a competition between transcriptional repressor (ICER) and transcription factor (CREB, cAMP response element binding protein) results in decreased IL-2 expression.

To sum up, cAMP expression results from activation of GPCR of AC by hormones or neurotransmitters [29]. This leads to immune suppression via GJIC of nT_{reg} to resT mediated by cAMP [36]. Consequently, modulation of the generation and degradation of cAMP is a promising approach to shape the immune response.

2.3 Characteristics of the non-nucleoside adenylyl cyclase inhibitor NKY-80

NKY-80 (2-amino-7-(2-furanyl)-7,8-dihydro-5(6H)-quinazolinone), displayed in Figure 4 is a non-nucleoside AC inhibitor [37]. According to the interrelation explained

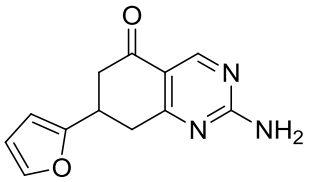

Figure 4: Structure of NKY-80

in chapter 2.2 it allows the regulation of the suppression of the immune system by attenuating the amount of expressed cAMP. NKY-80 is capable to interfere with the P-site (catalytic side) of the AC, which means binding to the same site as the substrate ATP [32]. However, the mode of inhibition is either un- or non-competitive as shown by kinetic analysis [38]. The inhibitor was discovered after virtual screening of more than 850,000 compounds on the basis of the pharmacophore analysis of AC and P-site ligands [37]. The focus of the initially research was put on inhibitors of the catalytic side, resulting in nucleoside-based compounds like THFA (9-(tetra-hydro-2-furanyl)-9H-purin-6-amine), also known as 9-THF-Ade [32]. These moieties bear a big disadvantage, the risk of interfering in DNA synthesis due to their structural similarity to nucleosides being the building blocks for the genetic material [32]. Unlike other studied compounds which have been listed by Seifert et al. in 2011, NKY-80 carries the properties of being a catalytic side inhibitor not containing an adenosine ring. Besides this drug, there is only MDL, also being

an AC inhibitor which is used for cell studies [39] holding the same features. In contrast to that, one drawback of NKY-80 is the lack in potency. IC_{50} values achieved in an AC assay in the presence of Mg^{2+} gave the following results displayed in Table 1.

Table 1: Overview of IC_{50} values of NKY-80 for three different isoforms of adenylyl cyclase, reported by two different references

	IC_{50} AC2	IC_{50} AC3	IC_{50} AC5
Iwatsubo et.al. [40]	2.6 mM	230 µM	15 µM
Onda et.al.[37]	1.7 mM	130 µM	8.3 µM

Due to the fact that this compound is of low potency, it is difficult to obtain fully saturated concentration/response curves for precise calculation of IC_{50} values explaining the deviation between the two sources [37].

2.4 Cell-penetrating peptides

Cell-penetrating peptides (CPP) are a group of peptides being capable of crossing the cellular membrane [41]. Since the first CPP, the transcription-transactivating (Tat) protein of HIV-1 has been discovered by Frankel and Pabo in 1988 [42], they are utilized in a diversity of applications like being attached to siRNA, nucleotides, small molecules, liposomes or proteins beyond others [43, 44], thus in case of a drug being coupled to a CPP a drug-delivery-system (DDS) is formed. Due to the difficulties in drug delivery, CPPs are a promising approach to overcome general problems in the administration of pharmacologically active substances [45]. The requirements for a drug being applied to an intracellular target site are oppositional to each other. They need to be both polar enough to ensure an easy administration and equal distribution and also show hydrophobicity to allow the penetration of the lipid bilayer of the cell [46]. This is the reason why several drugs fail to make it into clinical trials. To circumvent the necessity of extensive modification and fine-tuning in their final structure, connection to a CPP offers a promising alternative to ensure a good bioavailability [46]. In this way the potential therapeutic space can be expanded due to increased availability of targets [47]. CPPs, also referred to as protein-transduction domains (PTD) [44], typically consist of 5-30 amino acids, that can be divided into two groups depending on their binding properties. On the one hand are peptides requiring chemical linkage with the drug and on the other hand the ones forming stable, non-covalent complexes with the cargo [48]. Furthermore, they can be sorted

depending on their amino acid composition. CPPs containing several arginine or lysine residues represent the group of cationic CPPs. In contrast to that, also anionic or neutral sequences are possible. All of them vary in hydrophobicity and polarity, resulting in different modes of uptake. Furthermore, the level of uptake is dependent on diverse parameters like cell line, the cargo and the way it is attached to the CPP [49-52]. In general, different mechanisms of cell penetration are discussed extensively [53], as displayed in Figure 5.

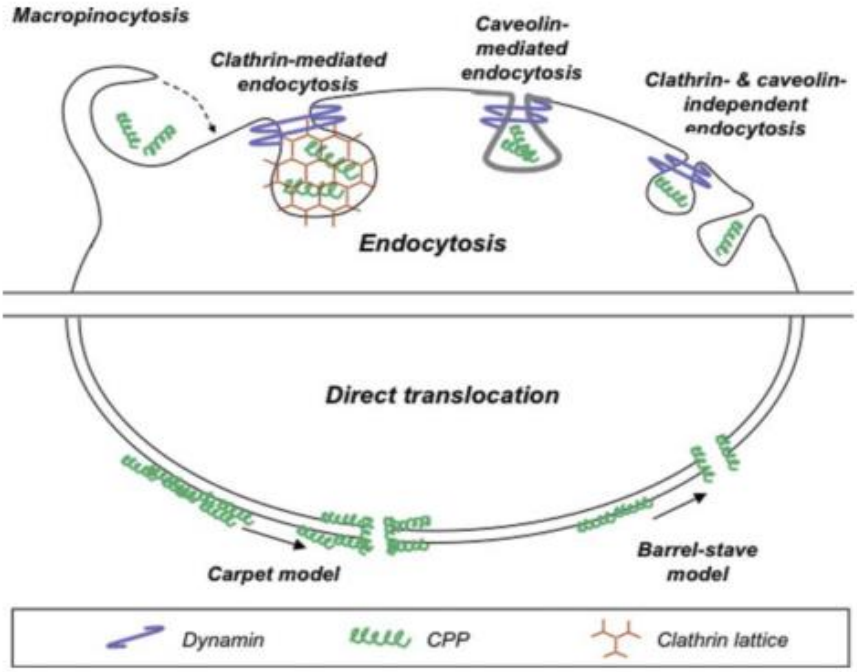

Figure 5: Different possible mechanisms of cellular uptake for cell-penetrating peptides [54]

Endocytosis and direct translocation are the major mechanisms explaining how substances are delivered into the cell. Endocytosis can further be split into clathrin-dependent endocytosis (CDE) and clathrin-&caveolin independent endocytosis (CDI).

In CDE, the cytoplasmic domains of plasma membrane proteins are recognized by adaptor proteins and packaged into clathrin-coated vesicles that are brought into the cell [55]. Due to the involved surface receptors this is the most selective form of endocytosis by that a CPP can enter a cell.

CDI is additionally divided in different forms, such as macropinocytosis, caveolae and/or lipid raft-mediated endocytosis. Macropinocytosis involves cell surface ruffling, providing a

relatively large cavity and thereby offer an efficient way for non-selective endocytosis of solute macromolecules [56]. Next, the formed macropinosome is carried along microtubules inside the cell [55]. In opposite to that, caveolae, a special form of lipid rafts, is mediated by a protein called caveolin, which is suggested to be responsible for stability of the membrane and shape of caveolae. Lipid rafts are microdomains present in the plasma membrane consisting of a combination of glycosphingolipids and protein receptors, being able to float freely in the membrane bilayer [57]. This mechanism is not well characterized and also referred to as nonclathrin/noncaveolar endocytosis [55].

In contrast to the endocytosis mediated delivery is the direct translocation. This mechanism in turn is divided in the carpet model and the barrel-stave model, differing in the organization of the membrane phospholipids. The carpet model describes an extensive reorganization of the previously mentioned membrane, whereas the barrel-stave model applies the formation of transient pores, resulting in a disturbance of the lipid bilayer. However, this model is not likely to occur for high molecular weight conjugates [58].

To sum up, all these pathways differ in their uptake mechanism but share a common result: extracellular substances are internalized into the cell after release of the plasma membrane by means of lipid vesicles [59]. Furthermore, they are harmless to the cells and do not destabilize the membranes or loose cellular integrity [58].

Whatever the case, the mechanism of delivery is strongly dependent on different parameters like the composition of the peptide or the cargo. With respect to this knowledge and experience, which physicochemical properties favor one mechanism over another, it will be possible to generate peptides following a certain uptake mechanism relevant to their application [54].

During this project, a peptide with the sequence Cys-Gly-Gly-Trp-Arg_8 has been used. Since octaarginin based proteins are well explored, it is assumed that this peptide is taken up by the cell via endocytosis instead of direct penetration. But still, the exact mechanism remains controversy and elusive [60]. Different assumptions are displayed in Figure 6.

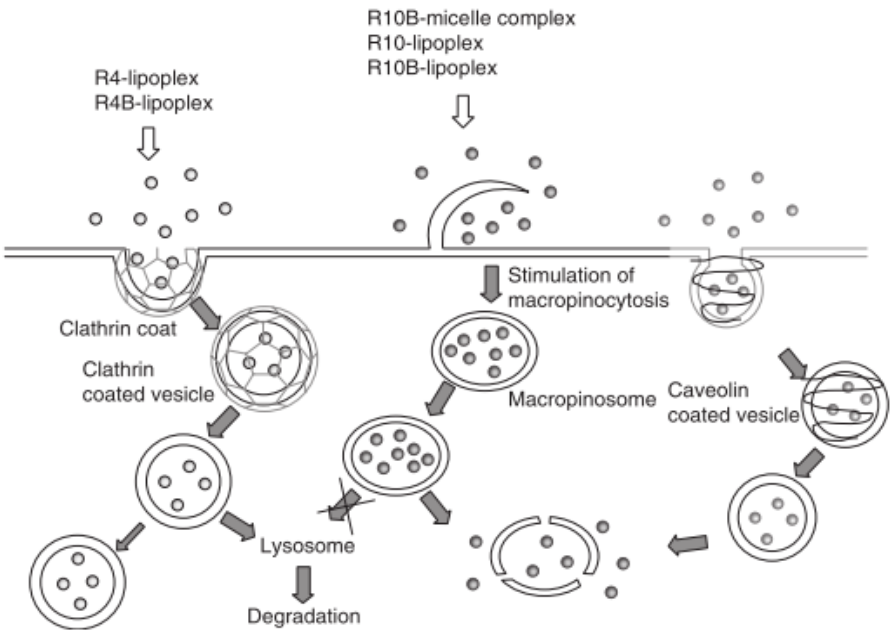

Figure 6: Different cellular uptake mechanisms in the case of oligoarginines depending on the chain length [60]. R4 and R10 describe the amount of repeated arginines, R4B and R10B stands for a different conjugation in contrast to R4 and R10.

As explained above, different endocytosis pathways are possible, like clathrin or caveolin coated vesicles, as well as macropinocytosis for bigger molecules consisting of longer arginine chains. Whatever uptake mechanism is carried out, the conjugate arrives inside the cell either as lysosome or is released into the cytosol.

Due to the change from physiological pH to acidic conditions in endosomes (pH 5.0-6.5) and lysosomes (pH 4.5-5.0) [10], the cargo can be cleaved from the CPP depending on the linkage. As in this project a hydrazone moiety is applied, which will be hydrolyzed at a pH lower than 6 [61]. This approach has already been reported by Kaneko et al. [62] for coupling a drug call doxorubicin to the linker applied in this project.

Beyond the beneficial properties of CPPs, there is also one big drawback being the imprecision in targeting, meaning all cells can be penetrated without distinction [44]. Nevertheless, cell-penetrating peptides offer a good strategy to deliver different types of cargos into cells and in case of drugs thereby reducing the applied dose and thus lowering the side effects.

2.5 Folic acid

Folic acid (FA) is an essential vitamin which is involved in DNA synthesis and therefore in cell proliferation [29]. Its structure is displayed in Figure 7 .

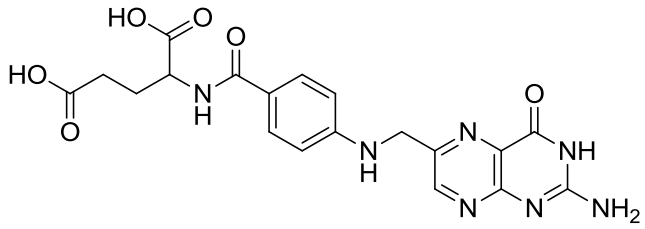

Figure 7: Structure of folic acid

It is synthesized by a couple of microorganisms before it is consumed by humans with their diet. After the uptake, the substance is reduced to active metabolites, whereof 5-Methyltetrahydrofolate is the most important one. Since the metabolites act as coenzymes during the transfer of carbon-moieties (e.g. methyl groups), they play a significant role in the synthesis of DNA-bases [63]. Due to this fact, quickly dividing cells require a higher amount of folic acid than normal cells do. This circumstance can be harnessed as targeting approach in cancer therapy, since cancer cells proliferate fast. To absorb the folic acid into the cell, special folic acid receptors are present at the cell membrane. Because quickly proliferating cells have a higher need of folic acid, they over express the corresponding receptor [16].

The absorbance mechanism of folic acid into the cell still remains unclear. However, it is assumed that it is mediated by endocytosis as displayed in Figure 8.

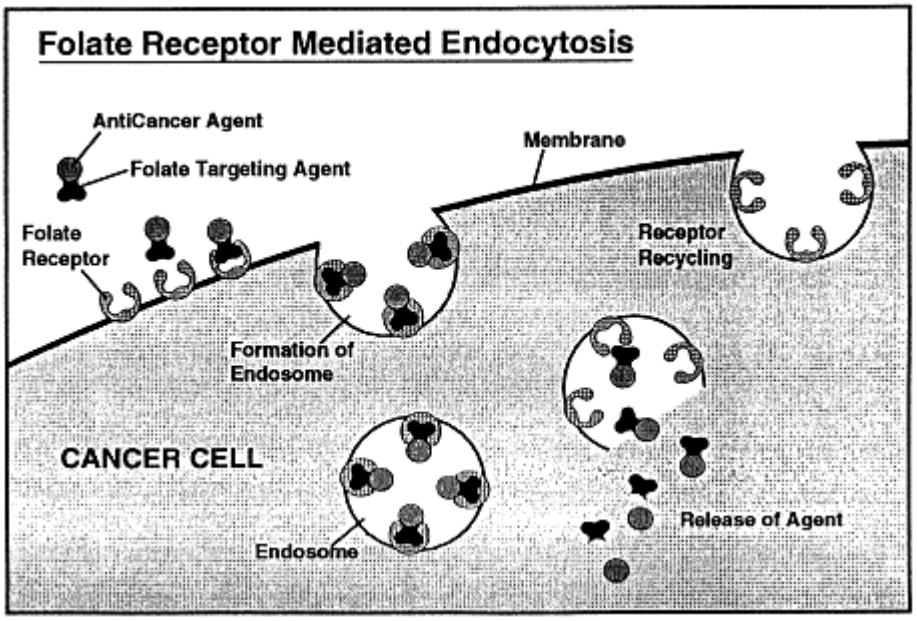

Figure 8: Uptake mechanism of folate conjugates via folate receptor [16]

According to this relation, anti-cancer drugs are coupled to folic acid derivatives to achieve a higher concentration of the drug inside the cell and without affecting healthy cells [17]. This procedure has been successfully applied for nanoparticles, protein toxins, anti-T-cell receptor antibodies, interleukin-2, chemotherapy agents, g-emitting radiopharmaceuticals, magnetic resonance imaging contrast agents, liposomal drug carriers and gene transfervectors [14]. The conjugation with folic acid bears several benefits as its small size, stability against temperatures and pH values making it capable for chemical modification, inexpensiveness, non-immunogenicity and its high affinity for binding to the folic acid receptor [64].

The figure shows the uptake of a folate-drug conjugate. First, the folate moiety is recognized by the folate receptor present at the membrane of the cancer cell. Next, an endosome is formed implicating the ligand-receptor complex. The endosome is transported to the inside of the cell, where it releases the folate-drug conjugate, which is decomposed resulting in free, uncoupled drug molecules. As displayed in the picture ambiguous, the endosome does not break within the cell. In case of the NKY-FA conjugate (conjugate of NKY-80 with folic acid), the hydrazone bond linking them together breaks within the acidic conditions inside the endosome, leading to release of the drug which is then small and hydrophobic enough to pass the endosome bilayer membrane.

This promising targeting approach is assumed to reduce the dose of the drug on the one hand and on the other hand limiting the side-effects.

3 Results and discussion

In order to influence the immune system to eradicate tumor cells, two final products have been synthesized during this project containing the adenylyl cyclase inhibitor NKY-80. On the one hand, it has been coupled with a cell-penetrating peptide to increase the cellular uptake since NKY-80 lacks in potency [37, 40]. The conjugate of CPP and NKY-80 could be applied by direct injection into the melanoma. On the other hand, NKY-80 was connected to folic acid. The second approach was done due to the folic acid receptors being present on cell membranes especially in higher amount on quickly dividing cells like melanoma cells. This fact can be used as targeting approach helping to decrease the applied dose of the drug and based on the selectivity of the folic acid to its receptor lowering the side-effects meaning affecting healthy cells. As displayed in Figure 9, a linker was synthesized bearing a hydrazine to couple the drug and furthermore offering a disulfide making it reactive against several possible coupling partners.

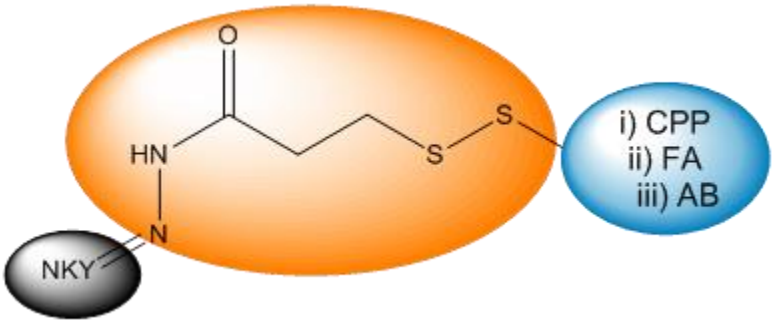

Figure 9: Structure of the linker (orange) coupled to NKY-80 (black) via hydrazone. Additional capability to bind different carriers (blue): i) CPP=cell-penetrating peptide, ii) FA=folic acid, iii) AB=antibody by forming a disulfide bond

A linker is necessary to bind NKY-80 to different carriers. The linker synthesized during this project, 3-(2-pyridyldithio)propionic acid hydrazide (PDPH), has been used for the coupling of different moieties, e.g. as described by Ansell et al. in 1996, conjugating an antibody with a liposome [65] or Zara et al. making immunoconjugates with the same linker [66]. It benefits of the presences of both, a hydrazine and an activated thiol. The first can form a hydrazone by reacting with a carbonyl-group as it is present in NKY-80. The activated thiol makes the coupling to other moieties offering a thiol possible, as in this project the conjugation with a cell-penetrating peptide and a modified folic acid, which are necessary to carry the drug into cells. Additionally, with this linker it would be possible to attach the drug to an antibody. The hydrazone bond ensures the release of the drug after internalizing into a cell. The internalization is mainly achieved by receptor mediated

endocytosis, thus resulting in the assumed formation of endosomes or lysosomes. Both bear an acidic environment within their compartment leading to cleavage of the hydrazone bond [61], thus free NKY-80 is present, which can then pass through the compartment into the cytosol. In case of another transportation pathway referred to as direct translocation, the drug-delivery-system ends up directly in the cytosol thus no change in pH will occur. However, the cytosol contains disulfide cleaving glutathione. Glutathione is a tripeptide present in almost all cells of the body, acting as antioxidants and disulfide reducing agent [67]. Consequently, the release of the drug is guaranteed, independent of the uptake mechanism into the cell, thus either the hydrazone or the disulfide is cleaved. Furthermore the bonds are stable within the blood stream to ensure the bioavailability at the point of action [68].

Chapters 3.1-3.4 discuss the single steps of the synthesis and a complete overview about the synthesis pathway performed is displayed in Figure 10.

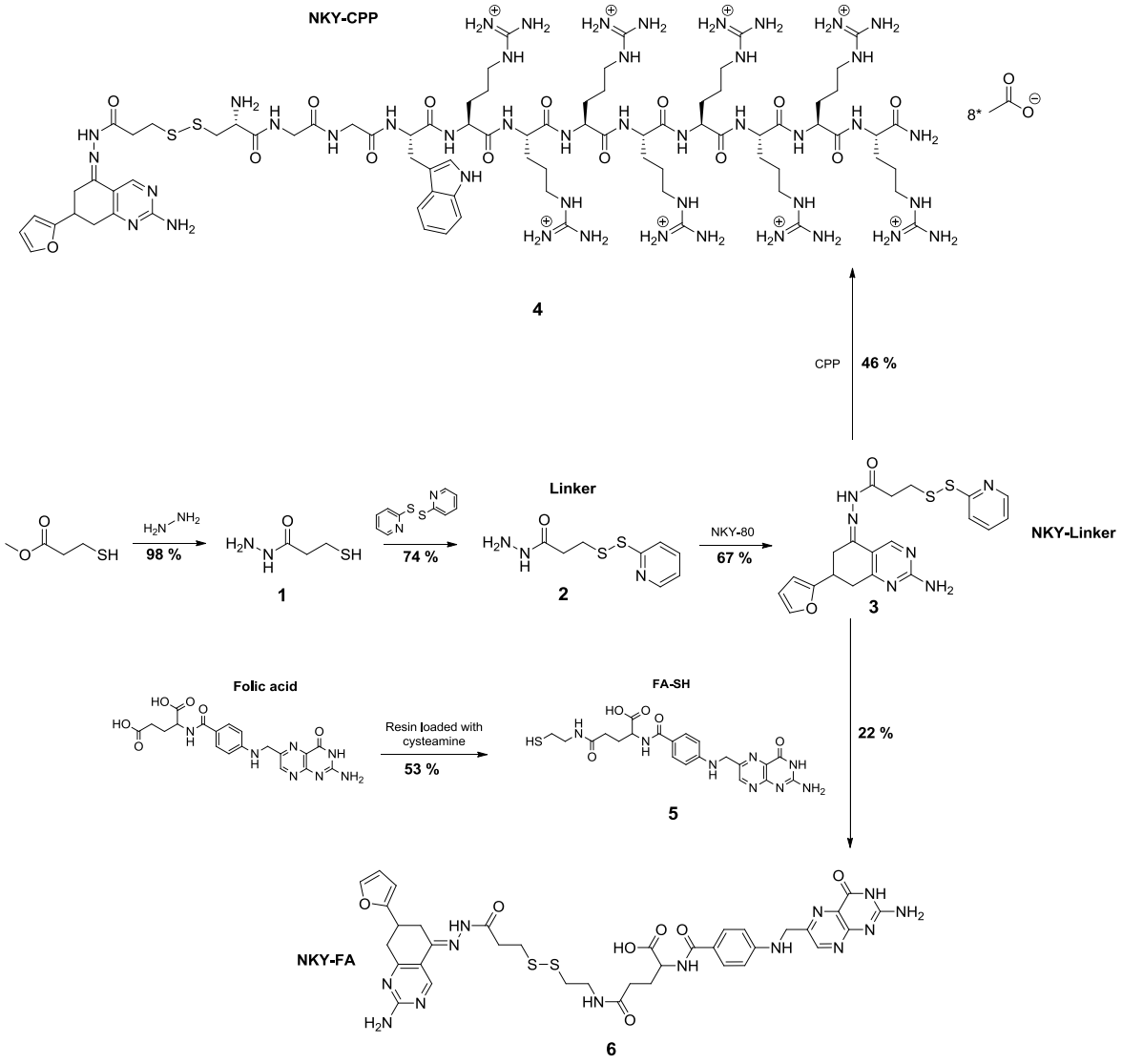

Figure 10: Complete overview about the performed synthesis

3.1 Linker synthesis

A linker containing two functionalities in order to be capable for coupling two different compounds was synthesized in a two-step reaction as displayed in Figure 11.

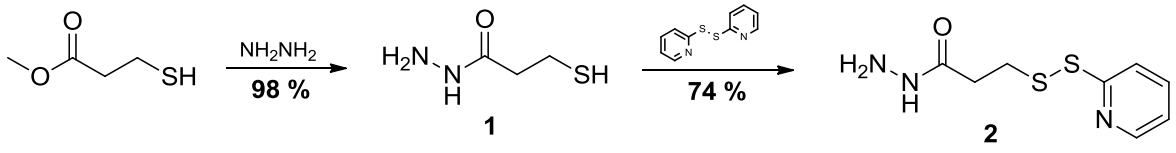

Figure 11: Two-step synthesis of linker bearing hydrazone and disulfide functionality making it capable of reacting with different moieties and couple them together

The first step reaction was carried out as described by Delius et al. in 2010 [69] resulting in a yield of 98 % and a purity of 95 %. The product was used without further purification for the second reaction step which was carried out in accordance to van der Vlies et al. in 2010 [70] and in house experiences. In opposite to the described procedure the product was purified using column chromatography, resulting in a slightly yellow solid with a yield of 74 %.

The synthesis of the cross-linker has been reported in literature, but using another pathway [66], starting from *N*,*N*'-bis(tert-butyloxycarbonyl)-L-cystine dimethyl ester forming the bis(hydrazide) by reacting with hydrazide. After protection of the hydrazide, the tetrakis-(BOC)cysteine derivative was formed which was then reduced to obtain the cysteine derivative. Next, the product was treated with 2,2'-dipyridyl disulfide to achieve the desired linker. The advantage of the reactions used in this project is the length, being short with two steps in opposite to 5 steps as reported. As reported by Zara et al. [66], the conversion with hydrazine yielded 87 %, the formation of the disulfide 53 %. Consequently, the conditions applied in this project do not only reduce the amount of work but also result in higher yields.

The structures of both obtained products (**1** and **2**) were confirmed using NMR spectroscopy (^{1}H and ^{13}C) and ESI-ToF-MS. For the first product, it is difficult to distinguish whether the disulfide or the free thiol has been formed. Directly after the synthesis of **1** has been performed, ^{1}H-NMR spectra were recorded in different solvents (DMSO-d_6 and $CDCl_3$). In both cases it was not clear if the free thiol is present due to the missing coupling between CH_2 and SH and the doubtful SH signal as displayed in Figure 12.

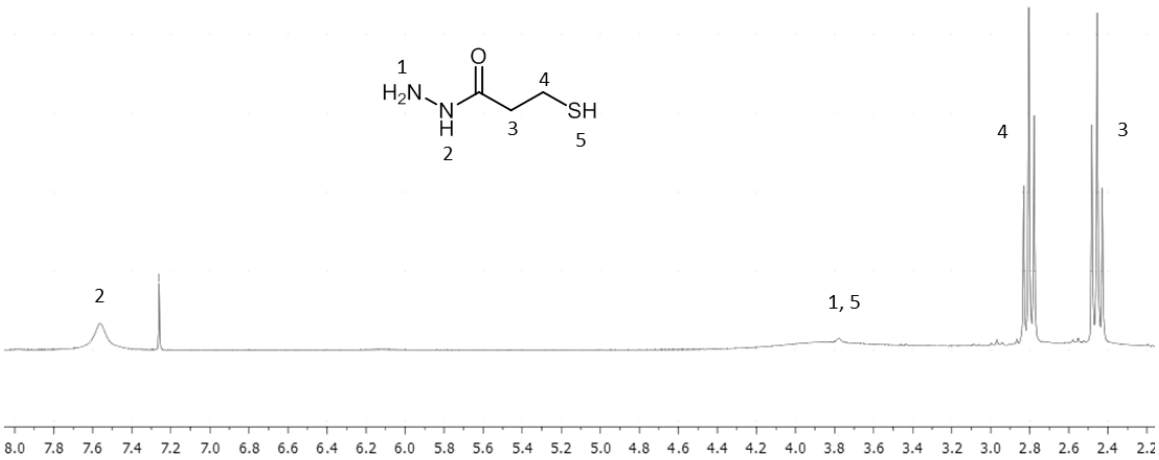

Figure 12: ^{1}H-NMR spectrum (250 MHz, $CDCl_3$, 298 K, reference: residual solvent $CHCl_3$) of 3-mercaptopropanehydrazide (1)

At a shift of around 3.8 ppm a hump is visible in the spectrum, possibly bearing signal 1 and 5. In comparison with literature data of 3-mercaptopropanehydrazide (**1**), the reported shifts for the CH_2-groups fit to the ones recorded. The compared spectra were measured in $CDCl_3$ [69]. The presence of the disulfide would influence the CH_2-S-group leading to a bigger shift difference between the two CH_2-groups (comparison with methyl-3-mercoptopropanoate and dimethyl 3,3'-dithiodipropionate, [71]). But since the shifts of the recorded and reported spectra fit, the presence of the free thiol is assumed. Additionally, for the two reference compounds, the shifts for carbons 3 and 4 vary when a disulfide is formed. In case of a free thiol, 4 can be assigned to a peak at around 20 ppm, 3 at around 38 ppm. After formation of a disulfide, both carbons would give peaks at around 33 ppm. The ^{13}C-NMR spectrum measured for compound **1** shows peaks at 20 ppm and 37 ppm, proving the presence of the free thiol.

The ESI-ToF-MS measurement of **1** was performed after some days of storage in the fridge while the high viscous oil change into a partly crystal structure. The mass showed the formation of disulfides. However, this aggregation can either have happened during storage or measurement. Nevertheless, the next reaction step could be carried out without problems.

The structure of **2** was confirmed by ^{1}H-NMR spectroscopy as displayed in Figure 13 as well as by ^{13}C-NMR spectroscopy (data not shown).

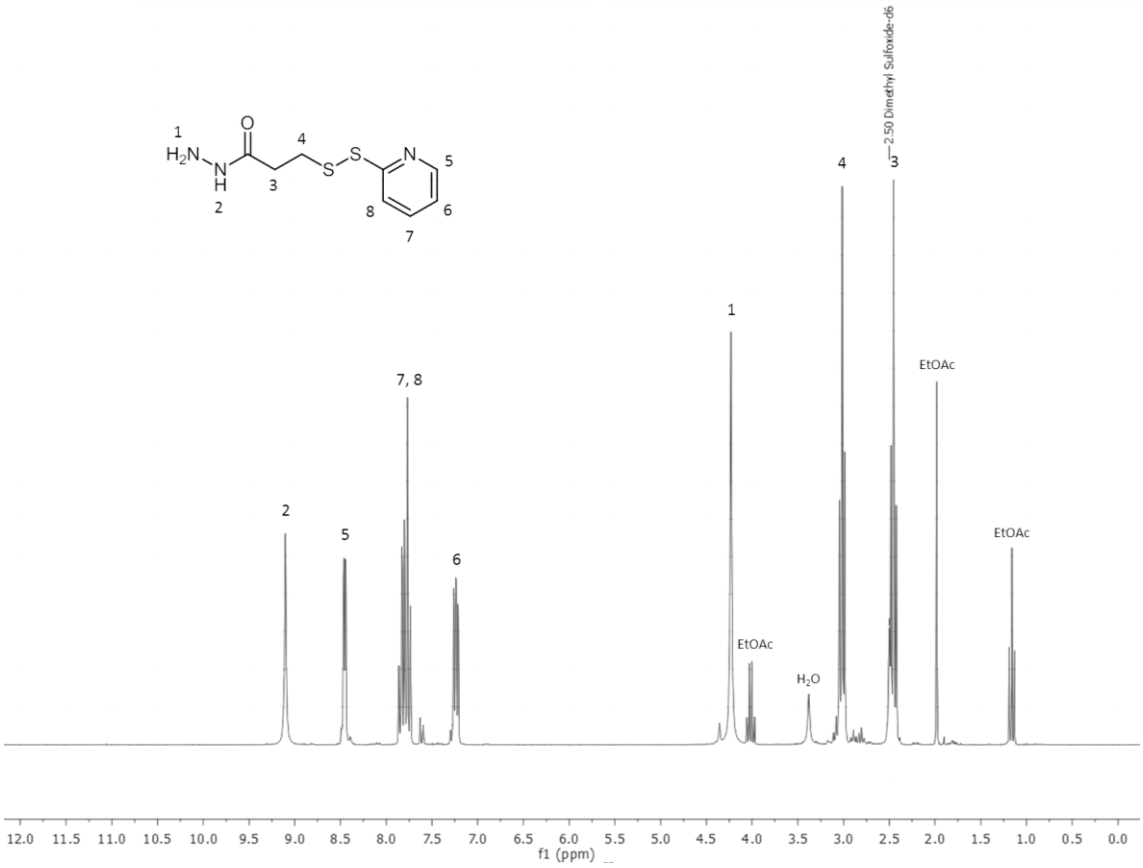

Figure 13: ^{1}H-NMR spectrum (250 MHz, DMSO-d_6, 298 K, reference: residual solvent DMSO) of product 2 confirming the desired structure

This NMR spectrum shows the four protons of the inserted pyridine moiety (number 5-8). The peaks 1-4 represent the groups that have already been present in the spectrum before, but after disulfide formation the CH_2 groups have shifted to low field.

This spectrum proves the successful reaction. This leads to the assumption, that **1** has been present as free thiol making the conversion to **2** possible. During the reaction 2-pyridinethiol is formed which tautomerizes to 2-pyridinethion, displayed in Figure 14, a yellow and stable molecule. The formation of this side-product is observed during reaction monitoring using TLC. In case of **1** has formed a disulfide, on the one hand the yellow compound could not be seen, and on the other hand the driving force of the reaction, the formation of the stable 2-pyridinethion, is lost. Although it could be thought about a disulfide-disulfide exchange reaction, it is not likely that this has happened in this case.

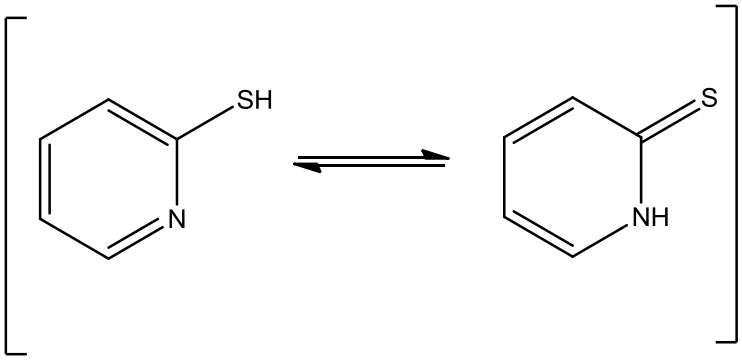

Figure 14: Tautomerism of the side product 2-pyridinethiol formed during the second step of the linker synthesis

The introduction of the 2-pyridinethiol group into the linker activates the thiol and being therefore beneficial for the following conjugation since it is additionally a good leaving group due to the above mentioned tautomerism.

The incomplete reaction proven by TLC led to the necessity of purification using column chromatography (solvent: EtOAc:MeOH 9:1, silica gel, pore size 0.04-0.063 mm). This process can simply cause loss of product due to mixed fractions. Furthermore loss during imprecise work can explain the yield of 74 %. Nevertheless, this process results in a pure product as also seen after recording an HPLC chromatogram showing 91 % purity.

ESI-ToF-MS spectrum displayed in Figure 15 shows the molecule peak as well as aggregates, adducts and fragments.

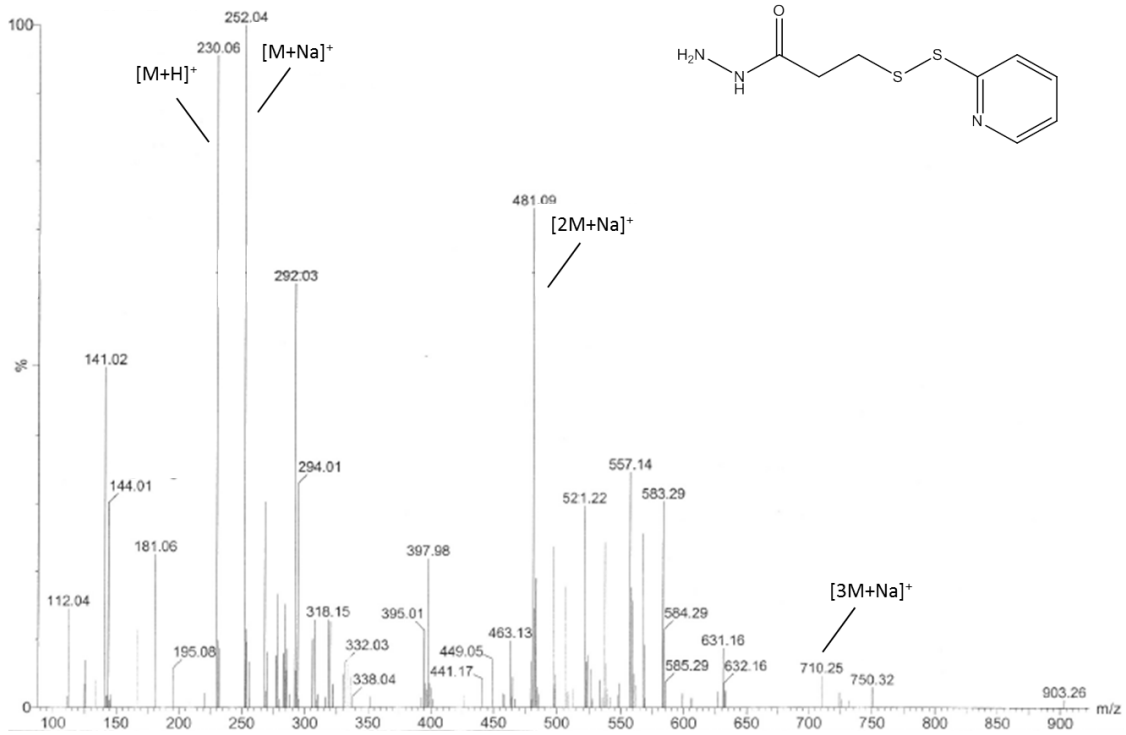

Figure 15: ESI-ToF-MS (positive mode) measurement of product of second step linker synthesis proving the structure by showing the protonated molecule peak, the corresponding sodium adduct, aggregates of two and three molecules as sodium adduct and one fragment as protonated and sodiated ion

The experimental and theoretical masses are displayed in Table 2. Furthermore the deviation in Da, as well as in percentage is shown. ESI-ToF-MS is a precise method giving results with an accuracy of about m/z ± 0.1, consequently the obtained results are satisfying and thus prove the correct mass of the product.

Table 2: Comparison of experimental and theoretical masses measured with ESI-ToF-MS for product 1. Molecular formula: $C_8H_{13}N_3O$, exact mass: 229.03 Da.

Peak	Experimental mass [Da]	Theoretical mass [Da]	Δmass [Da]	Deviation [%]
$[M+H]^+$	230.06	230.04	0.01	0.01
$[M+Na]^+$	252.04	252.02	0.01	0.01
$[2M+Na]^+$	481.09	481.05	0.01	0.01
$[3M+Na]^+$	710.25	710.08	0.02	0.02

The presence of the protonated molecule $[M+H]^+$ and its corresponding sodium adduct $[M+Na]^+$, besides the aggregates $[2M+Na]^+$ and $[3M+Na]^+$ confirms the structure of this reaction. Additionally, no peak with an m/z ratio of 120 is detected, proving the absence of **1**, the same applies for aldrithiol having an m/z ratio of 220 which is not identified within the above shown spectrum. However, the other peaks present in the spectrum cannot be assigned.

To sum up, both reactions led to the desired products which are confirmed by NMR spectroscopy and ESI-ToF-MS, furthermore the positive reaction within the next step proves the structures. The successful performances of these two reactions result in the linker being able to couple the drug to different carriers.

3.2 Coupling of linker to NKY-80

The linker, bearing a hydrazine moiety can be attached to the carbonyl-group NKY-80 as displayed in Figure 16.

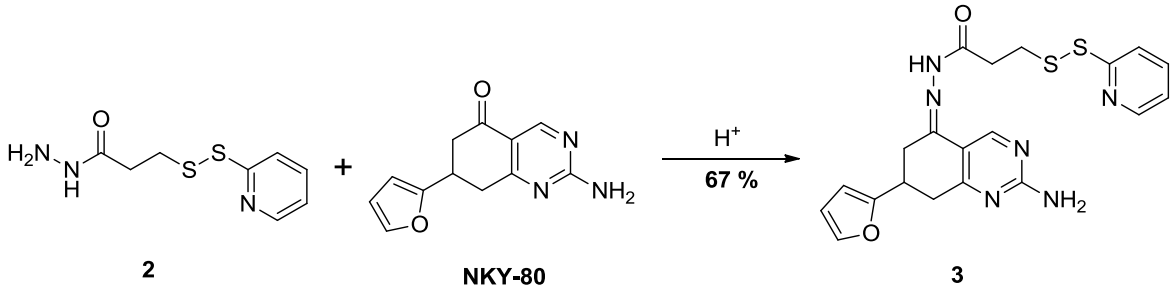

Figure 16: Coupling of linker to NKY-80 via hydrazone formation by reaction of hydrazine and keto-group

To find out the right conditions, the reaction was carried out three times. It was started with a ratio of 2:1 (**2**:NKY-80) and acetic acid as catalyst, since the TFA, which is used in literature [62], is a strong acid capable of cleaving the hydrazone bond. Since NKY-80 was not consumed completely, the equivalents of **2** were increased to 3, yielding in 57 %. During the second try, the reaction was additionally catalyzed with TFA, resulting in an increased yield of 62 %. When catalyzing the reaction with TFA only and using a ratio of 3:1 for **2**:NKY-80, the reaction yielded 67 %.

This conditions are similar to as reported by Kaneko et al. in 1991 [62] who used Doxorubicin in methanol. Since this exact reaction using NKY-80 has not been reported in literature, there is no reference to compare the yields. However, Kaneko et al. reported a yield of 90 % for the coupling to another drug called doxorubicin also via the formation of a hydrazone to the same linker as applied in this project. The loss can happen due to imprecise working.

During the formation of the hydrazone bond two isomers, E and Z, can be formed, which gets obvious when looking at the mechanism displayed in Figure 17.

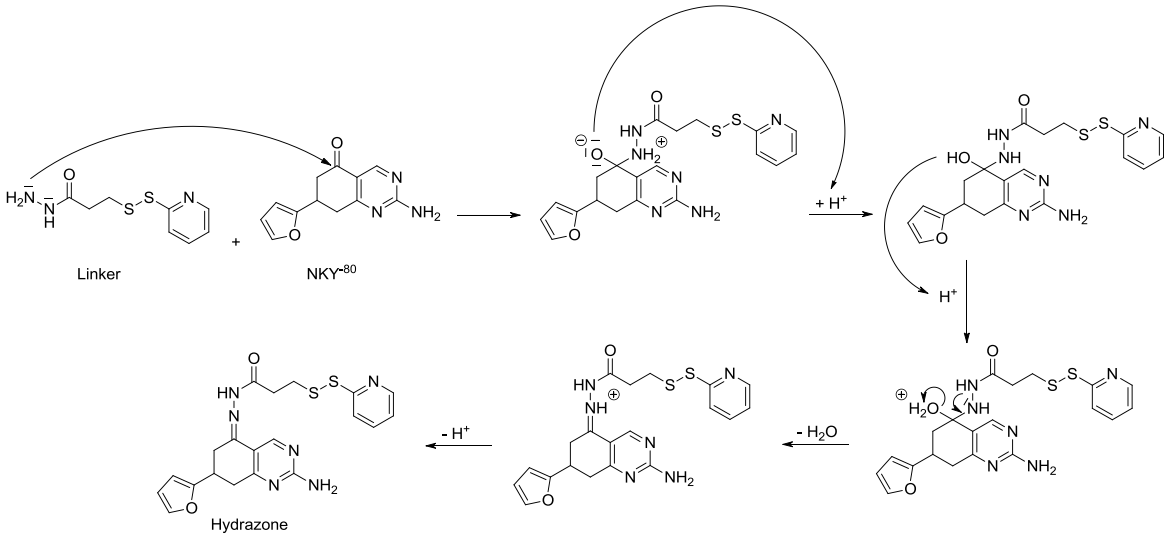

Figure 17: Formation of the hydrazone bond during the coupling of NKY-80 to linker

The lone pair of the hydrazine attacks the partial positive carbonyl atom of the NKY-80. After the formation of the nitrogen-carbon bond a negatively charged oxygen remains, taking up two protons which are acting as catalyst. Next, water is split off, resulting in nitrogen-carbon double bond carrying the positive charge. In this step it is decided whether the E or Z isoform is formed. By removal of the catalyst proton, a neutral molecule bearing a hydrazone bond is formed.

The assumption of two isomers is confirmed by NMR spectroscopy. As displayed in Figure 18, the ^{1}H-NMR spectrum shows two peaks for one proton in several positions in the low field.

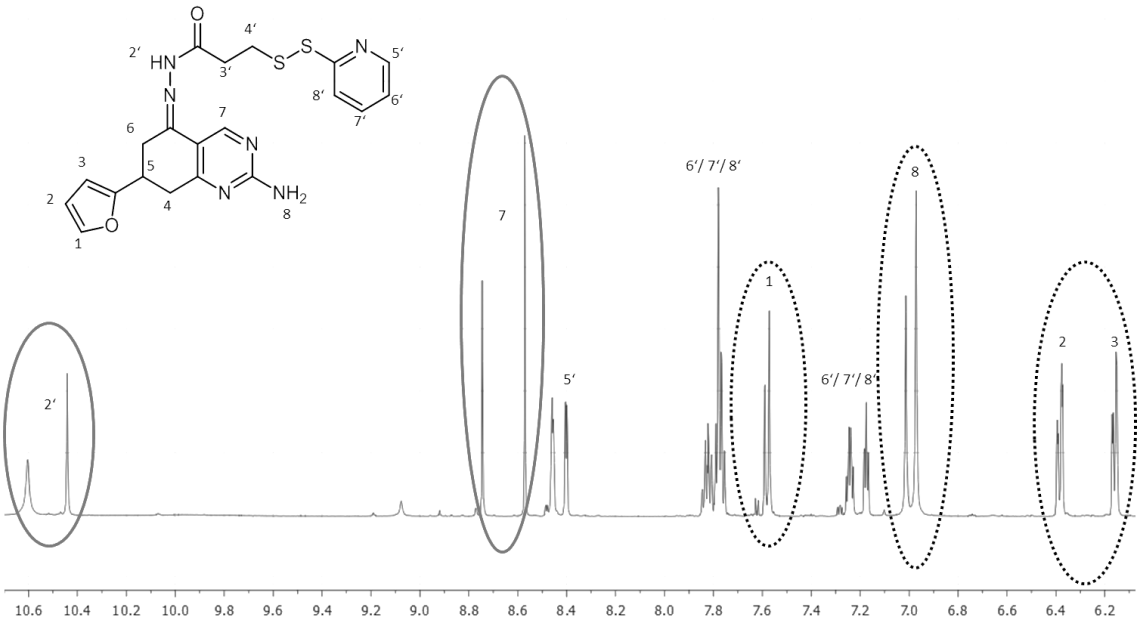

Figure 18: Cut-out of ^{1}H-NMR spectrum (700 MHz, DMSO-d_6, 298 K, reference: residual solvent DMSO) of the conjugation between linker and drug (3) for structure prove

The isomeric ratio is determined by integration of the peaks in circle in Figure 18 resulting in 0.4/0.6. Peaks belonging to proton 2' and 7 are highly influenced by the stereochemistry, resulting in higher shift differences. Peaks of proton 1, 2, 3 and 8 (dashed circles) are still influenced resulting in double peaks but giving almost the same shift. The influence gets obvious when comparing this spectrum with the one of unreacted NKY-80 where these double peaks do not appear. To sum up, the stereochemistry affects the whole molecule, however, due to overlapping, the stereochemistry cannot be proven for peaks of the pyridine ring and the ones appearing in high field. Furthermore, it is not possible to elucidate which peaks belong to which isomer.

An H-N correlation measurement further confirms the presence of E and Z isoforms. The NH group of the hydrazone bond is strongly influenced by the stereo chemistry inside the molecule. Consequently, two peaks can be assigned for the coupling between nitrogen and proton, which have almost the same shifts and together result with an area under the curve (AUC) of 1 in integration.

^{13}C-NMR spectroscopy, as well as 2D measurements were carried out to confirm the structure (data not shown).

TLC is used to monitor the reaction. In the reaction mixture, two spots are detected, referring to **2** and the new product. NKY-80 was completely consumed since no third spot

referred to NKY-80 is visible in the reaction mixture anymore. Although it has been converted completely, the reaction yielded 67 %. Compound **2** has been used in access explaining the presence of that spot in the reaction mixture. The elucidation if the new spot belongs to the desired product was obtained by different NMR measurements (see above), as well as ESI-ToF-MS and MALDI-ToF-MS. Both methods were applied to be absolutely sure to have the right product since this is the starting point for the following formation of the final products.

Figure 19 shows the ESI-ToF-MS spectrum.

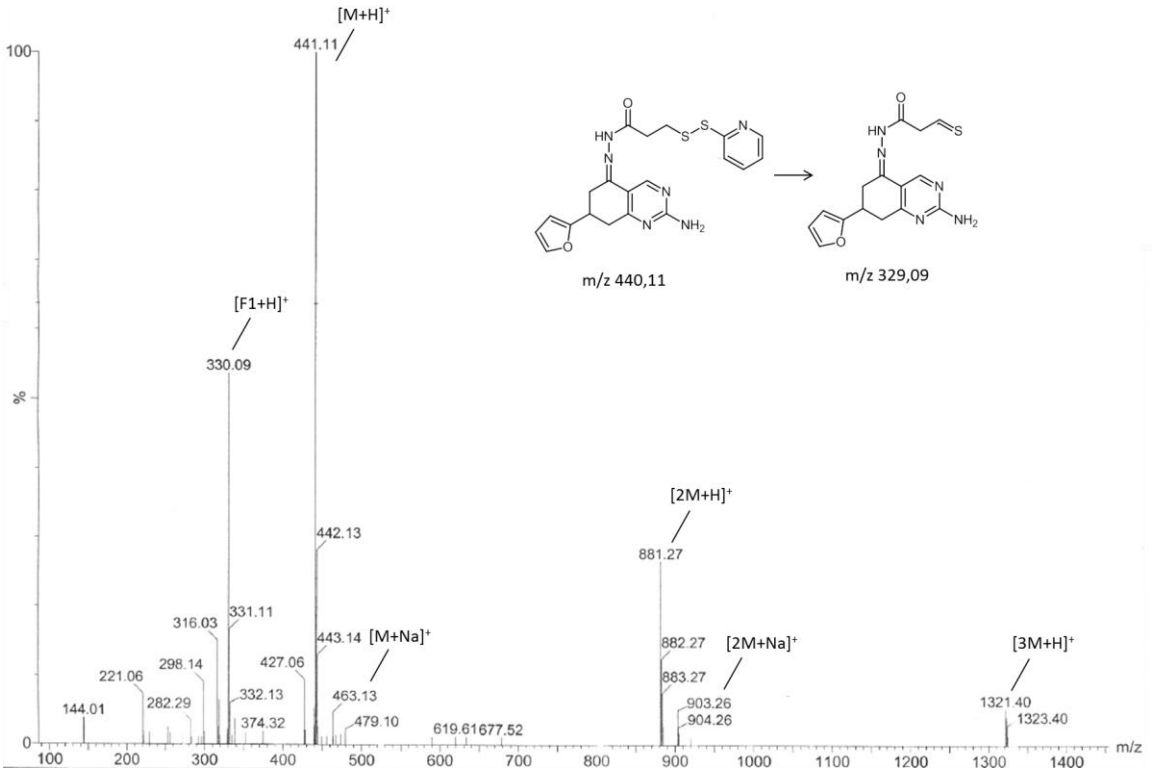

Figure 19: ESI-ToF-MS (positive mode) of NKY-linker conjugate (3)

The MALDI-ToF-MS spectrum shows the same masses (data not shown). Besides the protonated and sodiated molecule peaks ($[M+H]^+$, $[M+Na]^+$), double and triple aggregates are also visible ($[2M+H]^+$, $[2M+Na]^+$, $[3M+H]^+$). The disulfide bond is assumed to break during the measurement, but no fragment with a corresponding m/z of 331 can be detected. However, a significant peak at 330.09 marked as $[F1+H]^+$ is identified, which can be explained with a double bond formation between sulfur and carbon as also displayed within Figure 19.

Table 3 shows the experimental and theoretical masses for the assigned peaks, as well as their deviations from each other in Da and percentage. All peaks referred to the product show a very low deviation below 0.01 % and therefore prove the presence of the desired product.

Table 3: Comparison of experimental and theoretical masses measured with ESI-ToF-MS for product 3. Molecular formula: $C_{20}H_{20}N_6O_2S_2$, exact mass: 440.11 Da.

Peak	Experimental mass [Da]	Theoretical mass [Da]	Δmass [Da]	Deviation [%]
$[M+H]^+$	441.11	441.12	0.01	0.002
$[M+Na]^+$	463.13	463.10	0.03	0.007
$[2M+H]^+$	881.27	881.23	0.04	0.005
$[2M+Na]^+$	903.25	903.21	0.04	0.004
$[3M+H]^+$	1321.40	1321.34	0.06	0.005
$[F1+H]^+$	330.09	330.10	0.01	0.002

To conclude, NKY-80 was successfully coupled to the previous synthesized linker. Thus this conjugation now offers the opportunity of coupling the drug to either a cell-penetration peptide (see chapter 3.3) or a folic acid moiety (see chapter 3.4)

3.3 Coupling of NKY-80-linker to a cell-penetrating peptide

The NKY-linker conjugate, bearing a disulfide group can be attached the free thiol of cysteine being part of a cell-penetrating peptide as displayed in Figure 20.

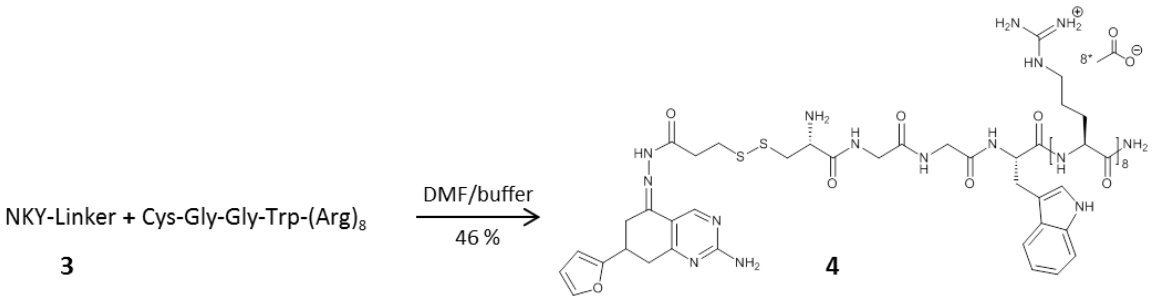

Figure 20: Coupling of linker-drug conjugate (3) to cell-penetrating peptide

The reaction was carried out as in a mixture of DMF and DPBS (Dulbecco's phosphate buffered saline) referring to in house experiences, resulting in a yield of 48 %. As explained for the formation of the linker in chapter 3.1, the driving force of the reaction is the formation of the side-product 2-pyridinethion pushing the equilibrium occurring during disulfide exchange to the product side. The buffer is necessary to ensure a constant neutral pH to avoid cleavage of the hydrazone bond.

The progress of the reaction monitored by HPLC and is displayed in Figure 21.

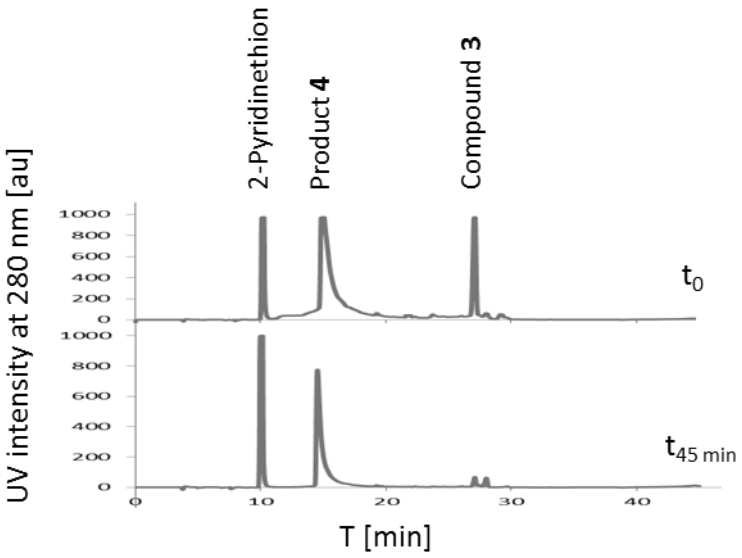

Figure 21: Progress of the coupling between NKY-80 and CPP measured by HPLC. X-axis: retention time in minutes, Y-axis: intensity measured with UV detector at 280 nm in atomic units

Immediately after mixing the two starting materials, a sample was taken. The according measurement is displayed in the upper line in Figure 21. It shows the starting material **3** and already formed product **4**. This shows the speed of the reaction, consequently, after 45 minutes the starting material is almost completely consumed. After 2 hours the ratio has not changed anymore thus purification using preparative HPLC was subsequently performed to remove the side product formed during the reaction, 2-pyridinethion and unreacted starting material. The free peptide cannot be detected in HPLC at the applied wavelengths, however ^{1}H-NMR of the product confirms the purity of the product and the absence of any starting material or side product.

Integration of the ^{1}H-NMR spectrum displayed in Figure 22 and exploitation of ^{13}C-NMR spectroscopy and 2D-NMR spectroscopy (data not shown) prove the successful coupling of the two compounds.

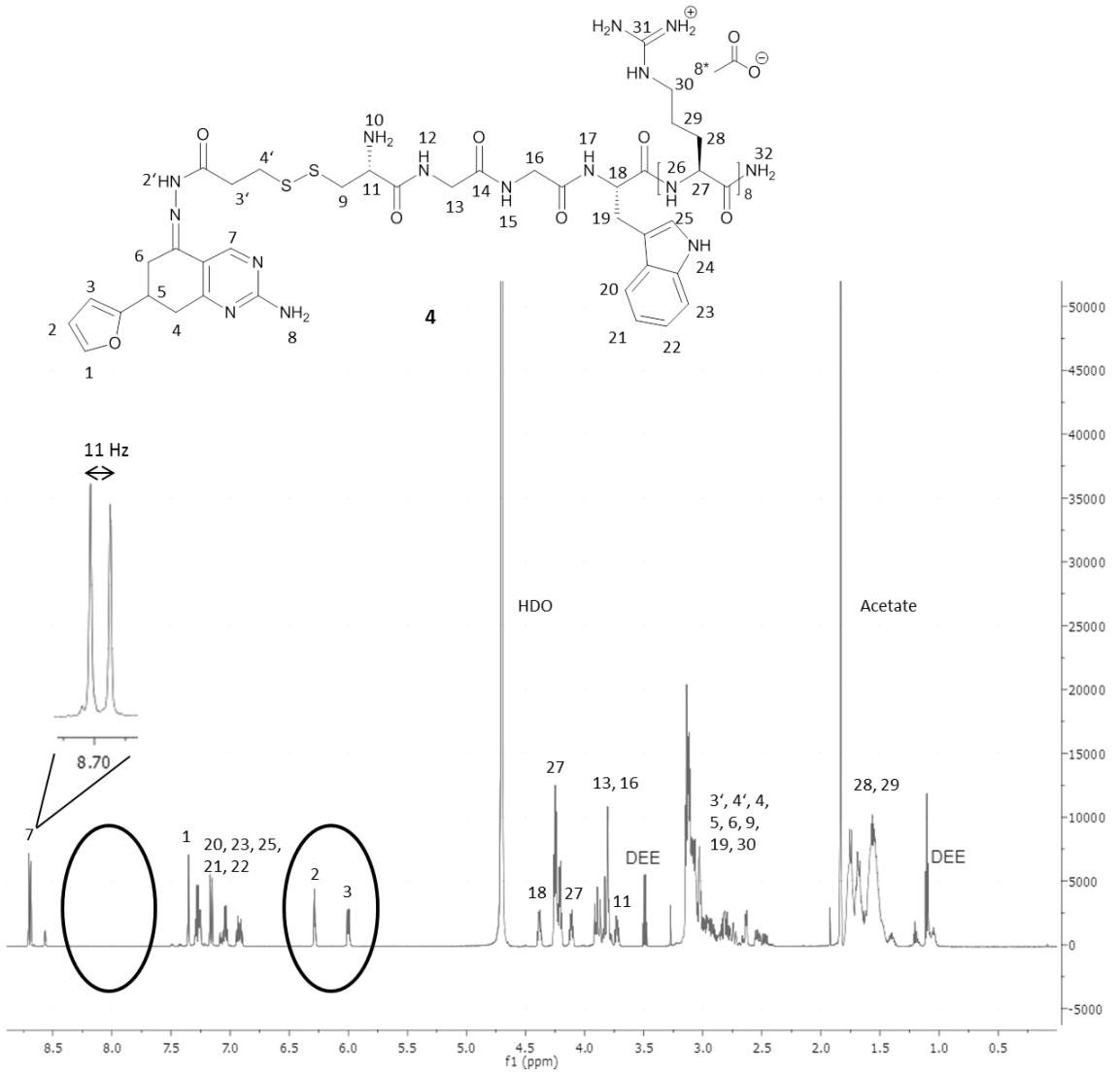

Figure 22: ^{1}H-NMR spectrum (700 MHz, D_2O, 298 K, reference: residual solvent HDO) of NKY-CPP conjugate as structure prove. DEE=Diethylether

The presence of the peaks 2 and 3 in the right circle confirms two of the protons of NKY-80. Additionally the disappearance of peaks (left circle) that would belong to the pyridine of the starting material NKY-Linker **3** makes sure that the reaction worked. Acetate is present due to the purification using HPLC where it is used as buffer and now offers the counter ion for the guanidinium groups. Diethylether is present because it is used for precipitation after purification. Acidic protons cannot be assigned due to the exchange with D_2O which has been used as solvent for the measurement.

The isomeric ratio observed for product **3** was 0.4/0.6. This shifted towards 0.5/0.5, showing that one isomer is more reactive than the other. However, the shift difference for the isomers is different than before. Isomers can be assigned for proton 7 (CH pyrimidine)

and proton 3 (CH furan). The shift difference for the two peaks referred to proton number 3 is small with 0.02, but similar to recorded for the conjugate with folic acid (see chapter 3.4). The peak difference between the two peaks assigned to proton number 7 is also small with 0.01. In contrast to that, for the drug-linker conjugate **3,** the peak difference is 0.28, in the folic acid conjugate it is 0.26. This means, that the influence of the isomericity of the molecule for the conjugate with the CPP is decreased. Nevertheless, the splitting can be detected, assuming the presence of both isomers, E and Z.

The mass is confirmed by MALDI-TOF-MS as displayed in Figure 23.

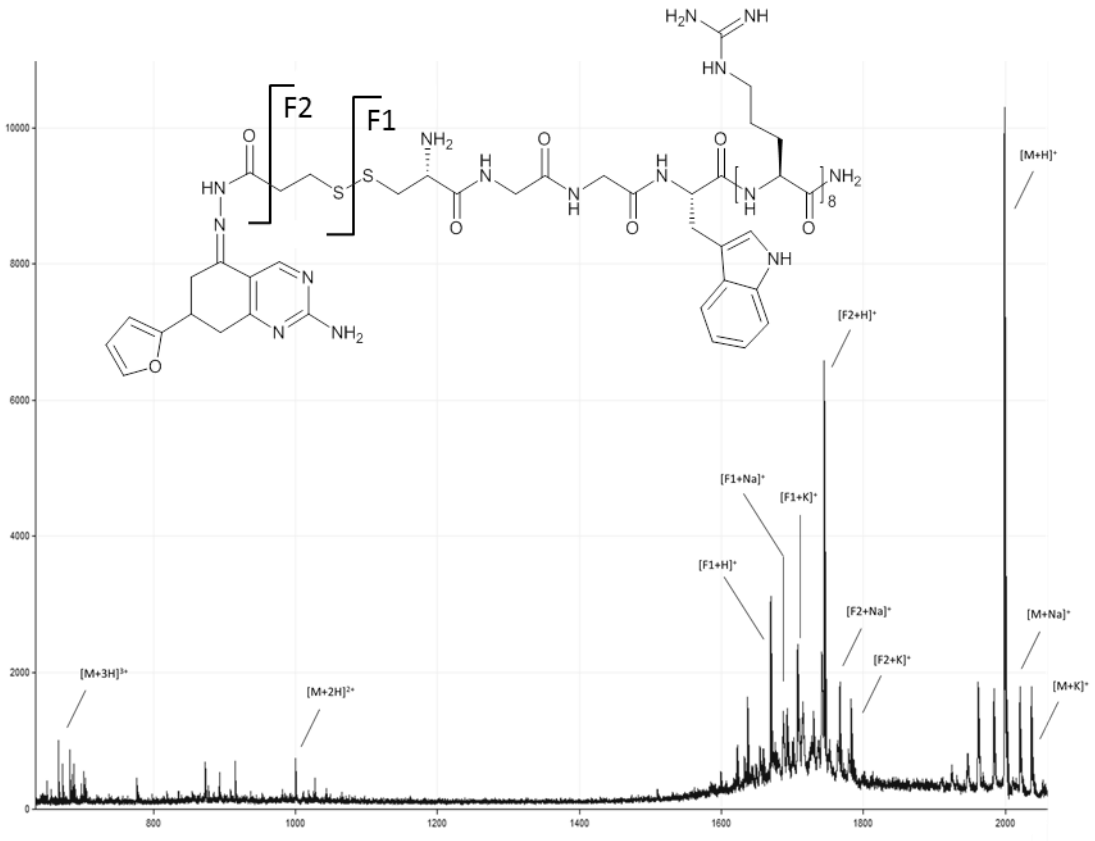

Figure 23: MALDI-ToF-MS spectrum of final conjugation of NKY-80 and CPP via linker. The spectrum shows singly and multiply charged product and different fragments

Not only the charged product ($[M+H]^+$), but also its sodium ($[M+Na]^+$) and potassium ($[M+K]^+$) adducts, as well as doubly ($[M+2H]^{2+}$) and triply ($[M+3H]^{3+}$) charged ions are visible. Furthermore two fragments ($[F1+H]^+$ and $[F2+H]^+$) with their sodium and potassium adducts are present. All assigned masses theoretically and experimentally are listed in Table 4.

Table 4: Comparison of experimental and theoretical masses measured with MALDI-ToF-MS for product 4. Molecular formula: $C_{81}H_{135}N_{43}O_{14}S_2$, exact mass: 198.06 Da

Peak	Experimental mass [Da]	Theoretical mass [Da]	Δmass [Da]	Deviation [%]
$[M+H]^+$	1999.42	1998.06	0.35	0.02
$[M+Na]^+$	2021.39	2021.05	0.34	0.02
$[M+K]^+$	2037.36	2037.16	0.20	0.01
$[M+2H]^{2+}$	999.99	1000.04	0.05	0.005
$[M+3H]^{3+}$	665.63	667.03	1,40	0.21
$[F1+H]^+$	1669.34	1667.96	1.38	0.08
$[F1+Na]^+$	1691.31	1689.94	1.37	0.08
$[F1+K]^+$	1707.23	1706.05	1.18	0.07
$[F2+H]^+$	1744.37	1742.0	2.39	0.14
$[F2+Na]^+$	1766.36	1764.0	2.40	0.14
$[F2+K]^+$	1782.33	1780.07	2.26	0.13

MALDI-ToF-MS shows a relative standard deviation of 0.1 % below m/z 20,000 when external calibration is applied as it is the case here [72]. All measured masses are within the standard deviation, thus proving the successful assignment of the peaks and therefore the structure of the desired product. It is positive to obtain low deviations also for higher masses since calibration is performed with standards of masses between 600 and 700 Da.

MALDI-ToF-MS is a sensitive method even being able to distinguish between different isotopes. As displayed in Figure 24, the isotopic pattern for the molecule peak is visible. The m/z difference between each peak results from the different amounts of C^{13} carbons compared to C^{12}, which have a relative probability of 1:99.

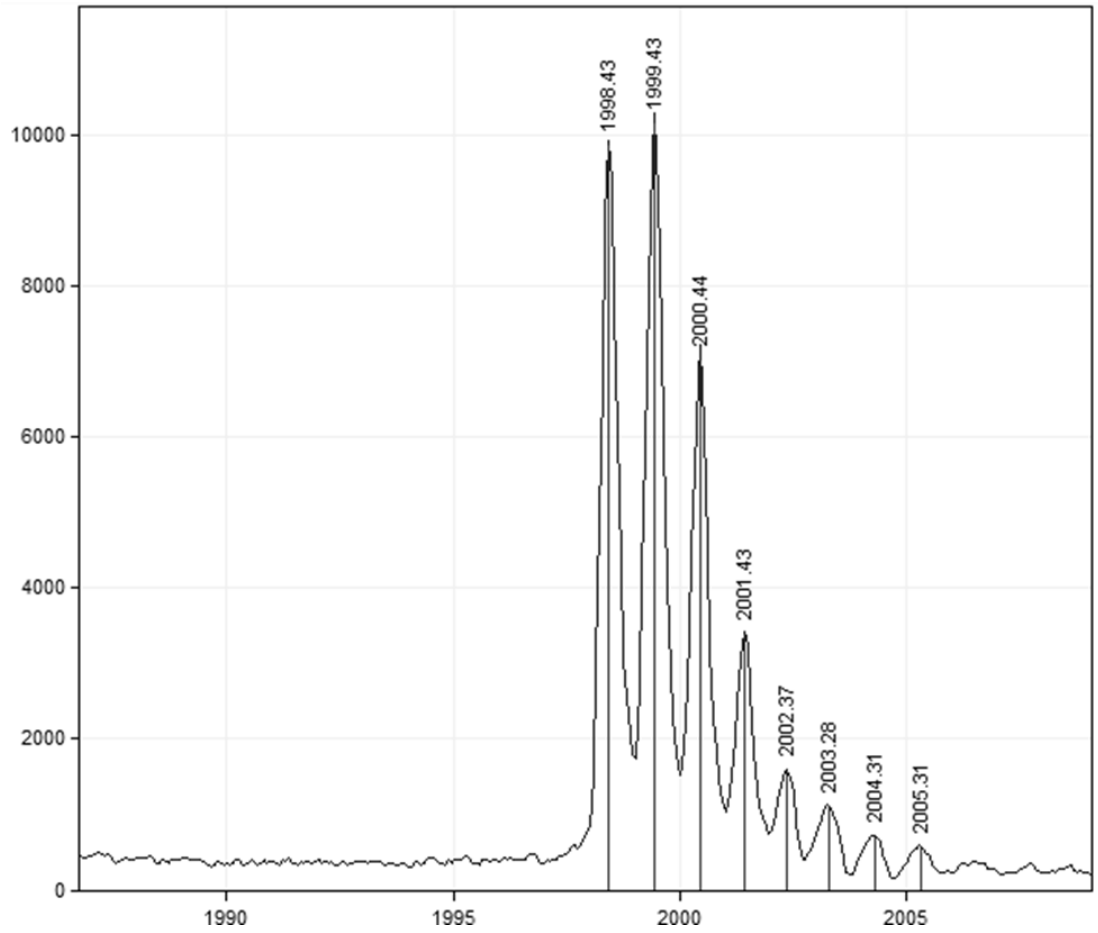

Figure 24: Isotopic pattern recorded by MALDI-ToF-MS of NKY-CPP product 4

The yield of 46 % can be explained by loss during purification using HPLC and imprecise work-up. Peptides have a secondary structure allowing it to fold itself. It is possible that due to the folding some cysteine groups are in the middle of the molecule thus sterically hindered and consequently not capable of reacting with NKY-linker **3**. Since this reaction is not known in literature, the yield cannot be compared to references.

In addition to the conjugation with the above mentioned CPP, it was tried to couple another CPP to **3** which was not successful due to insufficient quality of the peptide.

3.3.1 Stability test

To prove the stability of the NKY-CPP conjugate, it was placed in an environment with pH 5 and degradation was followed by HPLC.

NKY-CPP conjugate contains a hydrazone bond which ensures drug release from the carrier as a result of change in pH. This will occur when the conjugate enters a cell via

endocytosis. To confirm, that the bond will break when the conditions change, 0.4 M acetic acid was added to DPBS buffer to achieve a pH of ~5. To 150 µL of this solution, 1 mg NKY-CPP was added. Subsequently, the solution was measured using HPLC under the same conditions as used for purification of this product. The progress was checked after 1, 3, 7.5 and 24 hours. During that time, the quantity of the product peak decreased from 96 % at t1h to 93 % at t24h, whereas another peak which is related to NKY-80 without linker increased. The peaks were integrated to determine the quantity. The progress is displayed in Figure 25, showing the relative intensity of the peaks to each other at 280 nm. Besides NKY-CPP conjugate **4** and free NKY-80 another peak is visible having a similar retention time as NKY-Linker compound **3.** However, since disulfide bonds are stable at a pH of 5 and the peak does not change in intensity, this peak is referred to a system peak. In case this peak arises from compound 3, it would contain a hydrazone which would be cleaved at the acidic conditions resulting in decreased intensity.

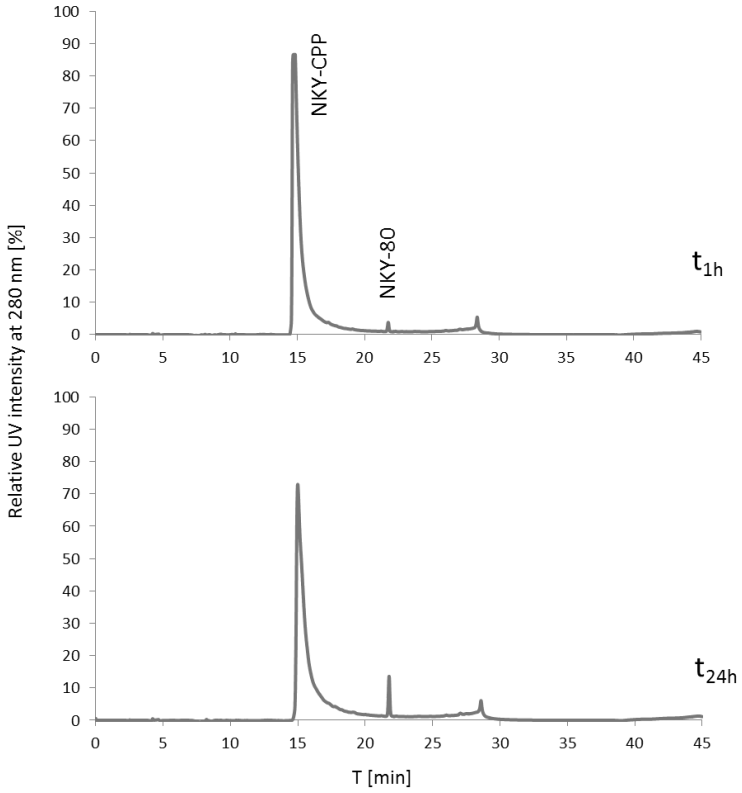

Figure 25: HPLC chromatogram displaying the cleavage of NKY-80-CPP conjugate at pH 5, measured after 1h and 24h. X-axis: Retention time in minutes, Y-Axis: relative UV intensity at 280 nm in %

The slow release of NKY-80 can be explained by the relatively low temperature. The experiment was carried out at room temperature, whereas inside the body a temperature of 37 °C would speed up the hydrolysis. The cleavage should be checked over a longer time to see if the NKY-80 is fully released. Nevertheless, the fact that NKY-80 is freed is of importance for the administration of this conjugation into the cell since the drug needs to be decoupled in order to react.

3.4 Coupling of NKY-80-linker to folic acid

The same NKY-linker conjugate as used in chapter 3.3 is applied for the conjugation of NKY-80 and folic acid, being a targeted approach for selective tissue penetration of melanoma cells. The conjugation between drug and folic acid was carried out as in a two-step reaction, the general pathway is displayed in Figure 26. For the first step, a solid phase support using a 4-methoxytitryl resin which was preloaded with 2-aminoethanethiol was applied. The reactants can diffuse into the pores of the resin reacting with the loading. This approach simplifies the work-up since all unreacted molecules can be washed away. Furthermore side-reactions are limited. After successful loading the conjugate is cleaved with acid.

Folic acid is added to obtain a conjugation between folic acid and cysteamine, which offers a free thiol which is necessary to be attached to the NKY-linker compound. This reaction resulted in an orange solid with a yield of 53 %.

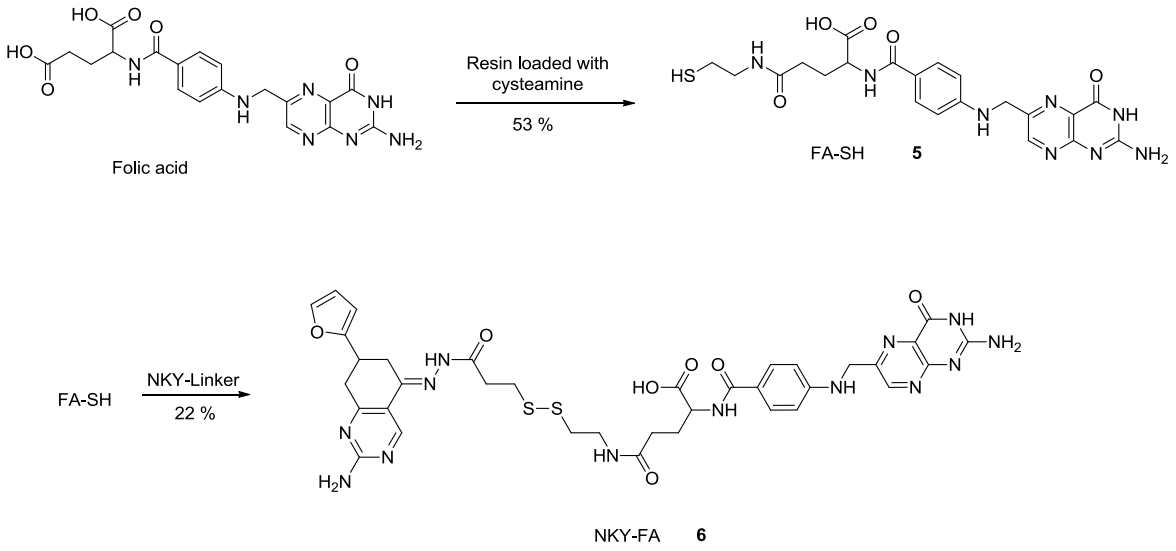

Figure 26: Modification of folic acid with cysteamine to introduce a thiol group and subsequent coupling to linker-drug conjugate

According to literature data [73], only one carboxy-group reacts, which can be explained by sterical preferences for this or sterical hindrance for the other group. Due to the solid phase, a doubly addition of cysteamine is not possible because auf sterical reasons. Nevertheless, an attachment to the other carboxy-group would not interfere with the

desire as the folic acid receptor will anyhow recognize the molecule, since the pteroate moiety is essential for receptor binding [64].

The structure of FA-SH (folic acid cysteamine) **5** was not entirely confirmed by ^{1}H-NMR spectroscopy, since the cysteamine protons are not doubtlessly assigned. Comparison with literature data proves the right allocation of the cysteamine peaks [73]. Additional NMR measurements (^{13}C and 2D) were carried out to prove the structure (data not shown).

ESI-ToF-MS and MALDI-ToF-MS were applied to confirm the mass. Both show $[M+H]^+$ and $[2M+H]^+$. In MALDI-ToF-MS the corresponding sodium and potassium adducts can be detected.

High resolution mass spectrometry confirms the molecular formula of FA-SH **5** as displayed in Figure 27.

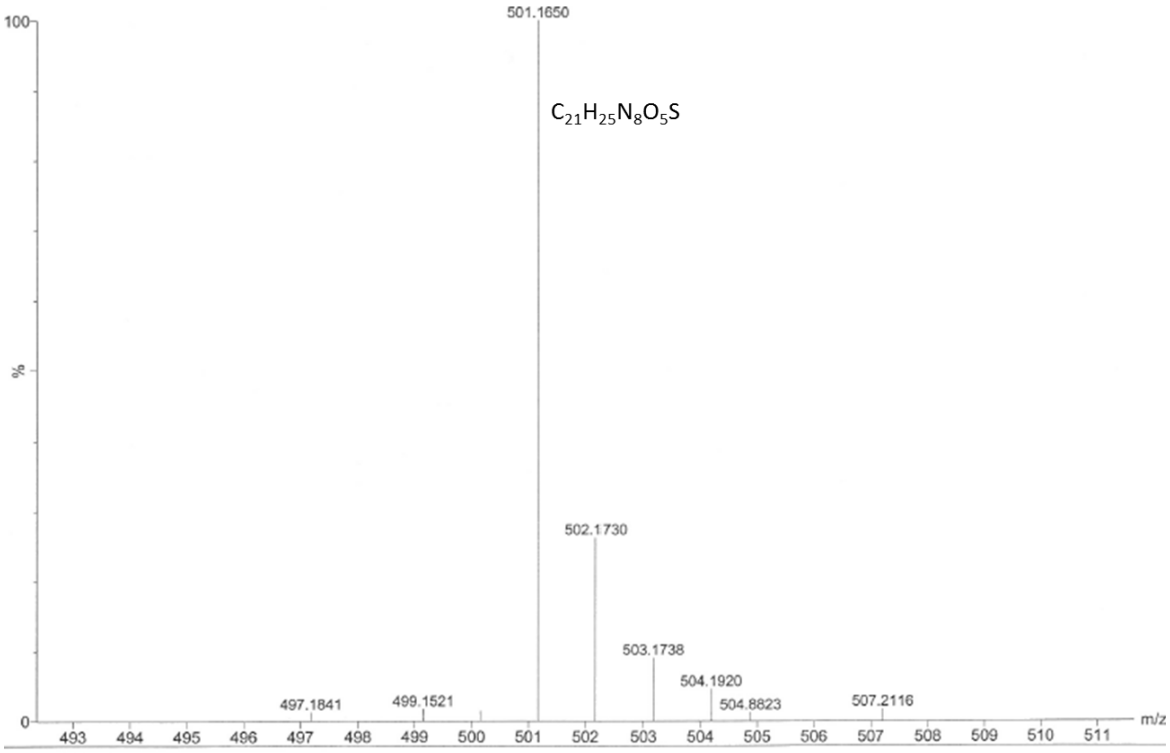

Figure 27: High resolution mass spectrometry analysis of product 5

The obtained folic acid derivative (FA-SH, **5**) now offers a free thiol which can react with the disulfide present in the NKY-linker conjugate. The whole reaction pathway is displayed in Figure 26. The conjugation of folic acid derivative **5** with NKY-linker **3** resulted in an orange solid with a purity of 60 %, thus a yield of 22 % is obtained.

NMR spectra (^{1}H and 2D measurements) of the conjugate of NKY-80 and folic acid confirm the structure (data not shown); also ESI-ToF-MS shows the mass of the product. However, ESI-ToF-MS as well as NMR spectroscopy assumes unreacted starting material to be present in the product. To check the purity of the compound, DOSY (diffusion-ordered-spectroscopy) was recorded. This proves the formation of the product and refutes the doubts if the ^{1}H-NMR is only a mixture of starting materials. In a DOSY measurement, the diffusion rate of a molecule is measured. Consequently, for each proton peak a diffusion rate is calculated, thus, all peaks within one molecule have the same diffusion rate since the whole molecule moves with the same speed. However, this measurement also confirms the presence of unreacted FA-SH **5**, since some peaks show two diffusion rates thus another molecule, starting material FA-SH **5** in this case, is underlying. This impurity has similar properties compared to the desired product and both are difficult to dissolve, thus purification of the resulting solid is complicated. As in this case only 12 mg were obtained, column chromatography would be challenging.
To sum up, the product is not pure and requires further purification and optimization of the reaction. Catalyzing the reaction with 0.3 equivalents Trifluoroacetic acid to push the reaction to completion and therefore avoid unreacted FA-SH **5** led to cleavage of the C=N bond between NKY-80 and linker. Nevertheless, the desired product was obtained but needs optimization in the future (see perspectives).

Prior the reaction using the loaded resin described above, an unloaded resin was used as described by Atkinson et al. [73]. The resin was swollen in DCM, next 2-aminoethanethiol was dissolved and added to the resin together with pyridine. After removal of the solvent and washing with DCM/pyridine, the conjugation with folic acid was carried out as described for the preloaded resin. However, the desired product could not be obtained. Since folic acid lacks in solubility, the solvent amount was increased compared to the literature which optimized the homogeneity of the solution but still did not result in the product. Either the loading of the resin did not work, even though a positive ninhydrin test proved the presence of primary amine, or cleavage of the product was not successful. In order to remove the possibly formed product from the resin, the amount of TFA was increased from three to 50 %, also not resulting in the product. It is assumed that the loading was not complete due to the relatively pale blue/violet color arising after ninhydrin test of the resin after attachment of 2-aminoethanethiol. Ninhydrin test of the preloaded resin in contrast gave a dark blue/violet appearance. Both tests were not quantified, but judged visually. This means, that the resin has been loaded but in a relatively small

amount, which could not be isolated after cleavage and work-up according to the procedure explained in literature [73].
To sum up, the desired product could not be obtained by using an unloaded 4-methoxytrityl resin, since the loading with 2-aminoethanethiol was too incomplete to achieve the desired product.

In addition to the solid phase support, it has also been tried to carry out reactions in solution using different conditions.
Referring to Zhang et al. [74], folic acid can be attached to cysteamine by forming and isolating the active ester of folic acid which should simplify the conjugation with 2-aminoethanethiol. Thus, a mixture of folic acid, *N*-Hydroxysuccinimide (NHS), *N*-*N*'-diisopropylcarbodiimide (DIC, coupling reagent, deviating from literature) and tiethylamine (TEA) was stirred for two days under argon in the dark, dissolved in DMSO. After filtration of a precipitate which is referred to a urea-derivative, precipitation in diethylether leads to a solid, which did not show the right structure in NMR spectroscopy.
Pasut et al [75] applied a similar procedure as described by Zhang et al. However, the work-up procedure is slightly different, furthermore this time dicyclohexylcarbodiimid (DCC) is used. After the reaction was poured into diethylether for precipitation as suggested in literature, it was placed in the fridge where the solution turned into a gel making further work-up impossible. The missing formation of a urea derivative confirms the unsuccessful reaction.
Another reference suggests a combination of DCC and 4-dimethylamiopyridine (DMAP) to form the NHS-ester of folic acid in DMSO. After stirring the mixture at 40 °C under argon atmosphere in a light-protected flask, a precipitate was formed which was filtered off. This precipitate is assigned to be a urea derivative which is always formed when working with DCC. Precipitation of the mixture in a cold solution of diethylether/acetone resulted in an orange solid. This compound shows a mass of 348.14 $[M+H]^+$ in ESI-ToF-MS when expecting m/z 538.47. Also the proton NMR spectroscopy did not confirm the structure of the NHS-folic acid. Nevertheless, it was tried to let this compound react with cysteamine, since the formation of urea showed at least a progress in the reaction, although the structure of the product remains unknown. The reaction with cysteamine was carried out referring to Pinhassi et al. [76]. The unknown product, cysteamine and diisopropylethylamine (DIPEA) are stirred together at room temperature under argon atmosphere in the dark overnight in DMSO. The mixture was then poured into diethylether/acetone to form a precipitate which was filtered off. Even though the reaction

was started with 150 mg, the amount obtained was not enough for a clear NMR spectrum. Nevertheless, the one recorded did not show the expected peaks.

Also a one-pot synthesis to obtain FA-SH has been carried out. Folic acid, 2-Succinimido-1,1,3,3-tetramethyluronium-tetrafluoroborate (TSTU) and DIPEA were dissolved in DMSO. After stirring for 3 h, cysteamine (2-aminoethanethiol) is added. The mixture was stirred over night at room temperature before it was poured into cold ether to form a precipitate. The obtained orange solid was checked with NMR spectroscopy and ESI-ToF-MS both not confirming the existence of the desired product.

To conclude, different combinations of coupling reagents and conditions for reaction and work-up have been tried all not resulting in the desired product. For unknown reasons the formation of either the NHS ester of folic acid or folic-acid-cysteamine was not successful.

4 Perspectives

Within this project two final products have been synthesized. On the one hand NKY-80 has been coupled to a cell-penetration peptide, on the other hand it is conjugated with a folic acid derivative.

Prior the testing in cell-lines, the stability of the products should be tested as described in chapter 3.3.1 over a longer period of time and at 37 °C to see whether the hydrazone is cleaved at an acidic pH as it would be present in endosomes or lysosomes after internalization into the cell.

Both of them should be tested in cell-tests to check their effectiveness. For the cell-tests, isolated immune-cells of mice and humans should be used. If effective, a murine-melanoma-model, as well as human immune-cells and human melanoma cells will be applied in immunodeficient mice, to check both, the uptake as well as the release of the drug. They will be done in collaboration with the institute of immunology, University of Mainz.

In case of NKY-CPP the potency of NKY-80 should be increased compared to free NKY-80. The conjugate containing folic acid first needs optimization in the synthesis before a pure product is obtained which should also be tested in cell-tests. For this optimization it is suggested to use an excess of NKY-Linker to avoid the presence of unreacted FA-SH, which is difficult to remove from the desired product due to similar properties. Furthermore the reaction should be carried out in bigger scale to obtain a greater amount of product to be able to purify it.

In addition to the coupling to a CPP and folic acid, NKY-80 should also be coupled to a suitable antibody that is also able to target regulatory T-cells and therefore also acts as targeting immunotherapy approach.

5 Summary

Adenylyl cyclase (AC) is a transmembrane protein which catalyzes the formation of ATP (adenosine triphosphate) to cAMP (cyclic adenosine monophosphate), which is a second messenger involved in diverse pathways. One function is the regulation of the immune response, since naturally occurring regulatory T cells ($nT_{reg}s$) maintain the suppression of the immune system by contact dependent communication with the responding T cells, where cAMP is transferred via gap junction intercellular communication (GJIC).

Melanoma cells overexpress cAMP and as a result the immune system is consequently suppressed allowing the cancer cells to proliferate in an uncontrolled way. The main aim of this project is to influence the activity of AC, which will decrease the level of cAMP in $nT_{reg}s$, leading to a reduced suppression of the immune response. In this approach, NKY-80 (2-amino-7-(2-furanyl)-7,8-dihydro-5(6H)-quinazolinone) is applied as potent adenylyl cyclase inhibitor. Due to the various functions of cAMP it is crucial to attach the AC inhibitor to a targeting compound ensuring to only affect the malignant cells without killing the other healthy cells. A suitable linker that was synthesized within this project which enables the attachment of the drug to several carrier molecules like i) a cell-penetrating peptide (CPP), ii) folic acid (FA), which was carried out during this project. The linker, which was synthesized in gram scale in good yields, bears two functionalities, on the one hand a hydrazine moiety being connected to the keto-group of the NKY-80 by forming a hydrazone bond and on the other hand offering a disulfide for the connection to the different carriers. The presence of a hydrazone allows the drug to be released in endosomes or lysosomes due to a decrease in pH (pH 5.0-6.5 or pH 4.5-5.0 respectively) leading to hydrolysis of the hydrazone bond. In case of the conjugate not entering the cell via endocytosis thus bypassing the endosomes and lysosomes, the disulfide bond will be reduced by glutathione, an enzyme being present in the cytosol.

NKY-80 was attached to a cell-penetrating peptide in milligram scale in order to increase the cellular uptake of NKY-80, which should enable the application of the conjugate in a locally administered dosage directly at the tumor side. Cell-penetrating peptides are a group of peptides that can cross the cell membrane by different mechanisms, either via endocytosis or direct penetration. However, this approach is limited to the direct injection of the conjugate into the melanoma, but not systemically, since it is not targeting the cancer.

Additionally, coupling to a folic acid moiety in miligramscale was carried out to enable the drug to affect only the quickly dividing cells, in systemic application, because they require a higher amount of folic acid for proliferation resulting in an increase in folic acid receptors on their outer membrane.

These two different approaches are promising ways on the one hand to increase the potency of the drug by binding it to a CPP and on the other hand to achieve a targeted delivery of the drug into melanoma cells by conjugation with folic acid.
To sum up, during this project a suitably linker with two functionalities was synthesized. After coupling NKY-80 to the linker via a hydrazone bond, both, a cell-penetrating peptide as well as a folic acid which was modified prior conjugation was attached to the linker via a disulfide bond. Both approaches will be tested in cell-tests in the future to check the effectiveness of the conjugation.

6 Zusamenfassung

Adenylylcyclase (AC) ist ein Transmembranprotein, das die Umsetzung von ATP (Adenosintriphosphat) zu cAMP (zyklisches Adenosinmonophosphat) katalysiert, welches ein sekundärer Botenstoff ist, der in diversen Signalwegen der Zelle involviert ist. Eine Funktion ist die Regulation der Immunantwort, da natürlich vorkommende regulatorische T Zellen ($nT_{reg}s$) die Unterdrückung des Immunsystems durch kontaktabhängige Kommunikation mit T Zellen regulieren, indem cAMP mittels sogenannter Gap-Junction-vermittelter interzellulärer Kommunikation (GJIC) transferiert wird.

Melanom-Zellen überexprimieren cAMP, woraus eine permanente Unterdrückung des Immunsystems resultiert, die es den Krebszellen ermöglicht, sich unkontrolliert zu vermehren. Die Grundidee dieses Projektes ist es, die Aktivität der Adenylatcyclase zu inhibiteren, was zu einer geringeren Menge an cAMP in $nT_{reg}s$ führt und somit die Unterdrückung des Immunsystems gemindert wird. In diesem Ansatz wird NKY-80 (2-Aino-7-(2-furanyl)-7,8-dihydro-5(6H)-quinazolinone) als potenter Adenylylcyclase-Inhibitor verwendet. Aufgrund der vielseitigen Funktionen von cAMP ist es notwendig, den AC Inhibitor an ein Molekül zu knüpfen, das diesen gezielt in maligne Zellen transportiert, um diese zum absterben zu bringen und gesunde Zellen am Leben lässt. Ein entsprechender Linker wurde hierfür synthetisiert, der es ermöglicht, den Wirkstoff an verschiedene Trägermoleküle wie Zell-penetrierende Peptide (CPP) oder Folsäure zu kuppeln, welches beides während dieses Projektes durchgeführt wurde. Der Linker, der in einer zweistufigen Synthese im Grammmaßstab in guten Ausbeuten synthetisiert wurde, enthält zwei Funktionalitäten, zum einen ein Hydrazid welches mit der Keto-Gruppe des NKY-80s zu einem Hydrazon reagieren kann, zum anderen ein Disulfid, welches die Kupplung zu Biomolekülen, die Thiolgruppen wie z.B. Cysteinreste enthalten, ermöglicht. Das vorhandene Hydrazon stellt die Abgabe des Wirkstoffs nach Eintritt in Endosome oder Lysosome sicher, da der verminderte pH (5,0-6,5 bzw. 4,5-5,0) das Hydrazon hydrolisiert. Falls die Verbindung in die Zelle nicht über Endozytose eintritt und somit die Endosome und Lysosome umgeht, kann das im Zytosol vorhandene Glutathion die Disulfidbindung reduzieren.

NKY-80 wurde im Miligrammmaßstab an ein Zell-penetrierendes Peptide gebunden um die Aufnahme in die Zelle im Vergleich zu freiem NKY-80 zu erhöhen, was somit die lokale Applikation direkt in den Tumor ermöglichen soll. CPP sind eine Gruppe von Peptiden die die Möglichkeit haben über verschiedene Mechanismen, entweder über

Endozytose oder direkte Penetration, in die Zelle einzudringen. Allerdings ist die Kupplung von NKY-80 zu einem CPP in ihrer Anwendung auf lokale Applikation limitiert, da CPPs nicht gezielt in Krebszellen aufgenommen werden, somit ist eine systematische Gabe ausgeschlossen.

Zusätzlich wurde NKY-80 im Miligrammmaßstab an Folsäure gebunden um den Wirkstoff gezielt in sich schnell vermehrende Zellen einzubringen, da diese einen höheren Bedarf an Folsäure haben und dadurch Folsäure Rezeptoren in vermehrter Menge an ihrer äußeren Membran präsentieren. Diese Kombination könnte systematisch angewendet werden.

Diese zwei Ansätze sind vielversprechende Wege um auf der einen Seite die Menge an NKY-80 in der Zelle zu erhöhen, indem es an ein CPP gebunden wird und auf der anderen Seite NKY-80, durch die Kupplung an Folsäure, gezielt in Melanom Zellen zu transportieren.

Während dieses Projekts wurde ein Linker mit zwei Funktionalitäten hergestellt. Nach der Kupplung von Linker und NKY-80 durch eine Hydrazonbindung wurde sowohl ein Zell-penetrierendes Peptid als auch eine zuvor modifizierte Folsäure über eine Disulfidbindung an den Linker geknüpft. Beide Ansätze werden in Zukunft in Zelltests auf ihre Effektivität getestet werden.

7 Experimental part

7.1 Instruments

NMR spectra were recorded on a Bruker Avance 250 MHz, Bruker AMX 300 MHz, Bruker DRX 500 MHz, Bruker Avance 700 MHz and Bruker Avance 850 MHz with the use of solvent proton signal as internal standard at 25 °C.

MALDI-ToF-MS analyses were performed using a Bruker Reflex II mass spectrometer (Germany) operating in the reflection mode. The instrument was equipped with a nitrogen laser (wavelength 337 nm) and spectra were recorded using a pulse rate of 3 Hz. Ions were accelerated by a voltage of 20 kV and detected by a micro channel plate detector. Calibration was carried out before each measurement using monoisotopic masses of fullerenes C_{60} and C_{70} at elevated laser power.

ESI-ToF-MS anylses were performed using a QToF Ultima 3 from micromass/waters.

Column chromatography was performed with silica gel 0.04-0.063 mm as the stationary phase with analytical grad solvents.

HPLC measurements were performed using a Jasco LC 2000 plus system equipped with PU-2086 Plus pumps, MD-2015 diode array detector and a ReproSil 100 C18 (250 x 4.6 mm) column with 5 µm particle size. Eluent A was water/TEAA (v:v 97.5:2.5), eluent B ACN. Applied gradient started with 0.0-35.0 min 0-70 % Eluent B, continued with 35-40 min 70-0 % Eluent B, and ended with 40-45 min 0 % Eluent B. The maximum pressure applied was 50.0 MPa, the injection volume was 20 µL, the measured wavelengths were 220, 280 and 340 nm, flowrate 1 mL/min.

Preparative HPLC was performed on the same system with a ReproSil 100 C18 (250 x 20 mm) column with 5 µm particle size and a flow rate of 1 mL/min.

7.2 Chemicals

Chemical	Purity and additional information	Supplier
Methyl-3-mercaptopropanoate	98 %	Sigma Aldrich
Hydrazine monohydrate	64-65 %, reagent grade 98 %	Sigma Aldrich
1,2-di(Pyridine-2-yl)disulfide	98 %	Alfa Aesa
NKY-80	N/A	VitasMLab, Ltd
Peptide	>80 %	Genosphere
Cysteamine 4-methoxytrityl resin	Loading: 0.20 – 1.30 mmol/g resin. Polymer matrix: copoly/styrene-1 % DVB, 200-400 mesh (DVB=Divinylbenzene)	Novabiochem
PyBOP	N/A	Novabiochem
DIPEA (*N*-Ethyldiisopropylamine)	99,5 %	Sigma Aldrich
Folic acid	98 %	Sigma Aldrich
Cysteamine hydrochloride	N/A	Fluka

7.3 Synthesis

3-Mercaptopropanehydrazide (1):

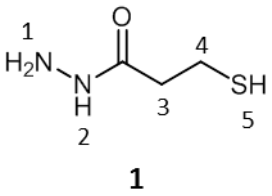

1

15.0 g (0.122 mol, 98 %) of methyl-3-mercaptopropanoate were dissolved in 20 mL methanol. 15.0 g (0.304 mol, 65%) hydrazine-monohydrate were dissolved in 25 mL methanol and added dropwise to the methyl-3-mercaptopropanoate within 1 h under argon atmosphere and room temperature. The colorless reaction mixture was stirred over night at room temperature under argon atmosphere. The solvent was removed under high vacuum resulting in a high viscous colorless oil with a yield of 98 % (14.7 g). ESI-ToF-MS: m/z 239.07 $[M+H]^+$ (disulfide), ^{1}H-NMR (250 MHz, DMSO-d_6) δ 9.05 (s, 1H, 2), 4.16 (s, 2H, 1), 3.26-2.78 (m, 1H, 5), 2.67 (t, J = 7.0 Hz, 2H, 4), 2.32 (t, J = 7.0 Hz, 2H, 3). R_f 0.23.

3-(pyridine-2-yl-disulfanyl)propanehydrazide (2):

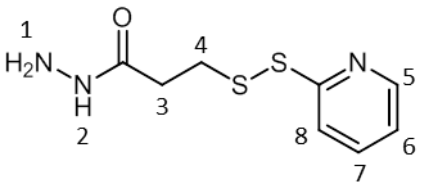

2

5.00g (22.2 mmol, 98 %) of 1,2-di(pyridine-2-yl)disulfide were dissolved in 30 mL Methanol. 1.36g (10.8 mmol, 95 %) **1** were dissolved in 20 mL methanol and added to the solution of 1,2-di(pyridine-2-yl)disulfide dropwise under argon atmosphere and room temperature. The yellow reaction mixture was stirred over the weekend at room temperature under argon atmosphere. After monitoring the reaction with TLC (solvent EtoAc:MeOH 9:1) the mixture was purified on column chromatography (solvent: EtOAc:MeOH 9:1, silica gel, pore size 0.04-0.063 mm) resulting in a colorless solid with a yield of 74 % (2.00 g). ESI-ToF-MS: m/z 230.06 $[M+H]^+$. ^{1}H-NMR (250 MHz, DMSO-d_6) δ 9.10 (s, 1H, 2), 8.45 (ddd, J = 5.0, 2.0, 1.0 Hz, 1H, 5), 7.88 – 7.71 (m, 2H, 8, 7), 7.24 (ddd, J = 7.0, 5.0, 1.0 Hz, 1H, 6), 4.23 (s, 2H, 1), 3.02 (t, J = 7.0 Hz, 2H, 4), 2.45 (t, J = 7.0 Hz, 2H, 3). R_f value: 0.32.

***N*'-(2-amino-7-(furan-2-yl)-7,8-dihydroquinazolin-3(6H)-ylidene)-3-(pyridin-2-yldisulfanyl)propanehydrazide (3, NKY-Linker):**

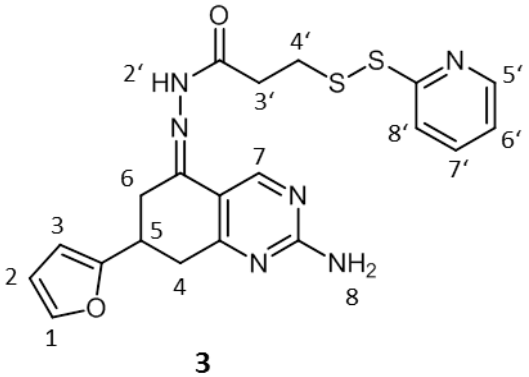

3

1.05 g (4.17 mmol, 91%) **2** and 0.350 g (1.51 mmol, 99 %) 2-amino-7-(furan-2-yl)-7,8-dihydroquinazolin-5(6H)-one (NKY-80) were dissolved in 35 mL chloroform under argon atmosphere and room temperature. 0.01 mL (0.15 mmol) trifluoroacetic acid (TFA) were added dropwise to catalyze the reaction. The reaction was stirred under argon atmosphere at room temperature overnight. After monitoring the reaction with TLC (solvent: EtOAc:MeOH 9:1) showed completion of reaction, the solvent was almost completely removed, the precipitate was filtered off and dried under high vacuum resulting in a slightly yellow solid with a yield of 67 % (510 mg). ESI-ToF-MS: m/z 441.11 $[M+H]^+$, ^{1}H-NMR (700 MHz, DMSO-d_6) δ 10.60 (s, 0.6H, 2')*, 10.44 (s, 0.4H, 2'), 8.74 (s, 0.4H, 7), 8.57 (s, 0.6H, 7)*, 8.46 (d J = 4.5 Hz, 0.6H, 5')*, 8.40 (d, J = 4.5 Hz, 0.4H, 5'), 7.86 – 7.74 (m, 2H, Py), 7.59 (d, J = 1.5 Hz, 0.4H, 1), 7.57 (d, J = 1.5 Hz, 0.6H, 1)*, 7.24 (m, 0.6H, Py)*, 7.18 (m, 0.4H, Py), 7.01 (s, 0.8H, 8), 6.97 (s, 1.2H, 8)*, 6.39 (dd, J = 3.0, 1.5 Hz, 0.4H, 2), 6.38 (dd, J = 3.0, 1.5 Hz, 0.6H, 2)*, 6.17 (d, J = 3.0 Hz, 0.4H, 3), 6.15 (d, J = 3.0Hz, 0.6H, 3)*, 3.15 – 2.53 (m, 9H). R_f value: 0.57. *=Signals of major isomer

NKY-Linker-Cys-Gly-Gly-Trp-$(Arg)_8$*8Ac (4):

5 mg (10.0 µmol, 88 %) of **3** was dissolved in 3 mL DMF. 44 mg (17.03 µmol, 80 %) of the peptide CGGWRRRRRRRR*8TFA (amidated C-terminus) were dissolved in 1 mL DPBS buffer (Dulbecco's phosphate buffered saline) and added to the solution at room temperature dropwise. The reaction was monitored using HPLC (solvent:97.5% H_2O/2.5 % TEAA:ACN, column: C-18). After disappearance of **3** after 2h, the mixture was purified using preparative HPLC. The combined fractions were lyophilized, the crude was dissolved in 1 mL methanol and poured into 100 mL diethylether resulting in a colorless solid with a yield of 46 % (12.0 mg) and a purity of 96 %. MALDI-ToF-MS: m/z 1999 $[M+H]^+$. Isomeric ratio of hydrazone bond

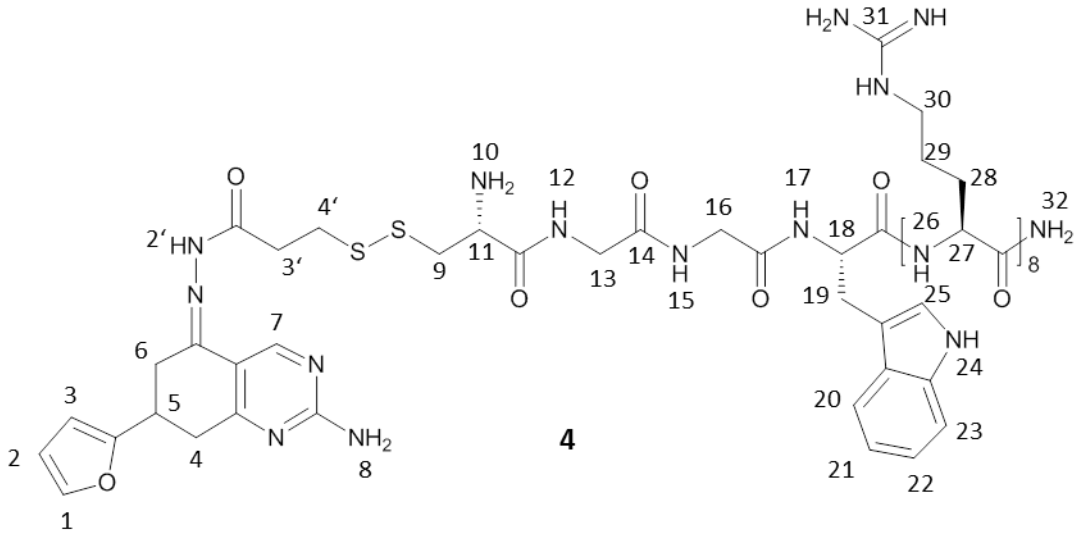

0.5/0.5: ^{1}H-NMR (700 MHz, D_2O) δ 8.70 (s, 0.5H, 7), 8.69 (s, 0.5H, 7), 7.35 (s, 1H, 1), 7.29 (d, *J* = 8.0 Hz, 1H, 20), 7.26 (dd, *J* = 8.0, 4.0 Hz, 1H, 23), 7.16 (d, *J* = 11.5 Hz, 1H, 25), 7.04 (m, 1H, 21), 6.92 (m 1H, 22), 6.30 – 6.27 (dd, *J* = 3.0, 1.5 Hz, 1H, 2), 6.01 (d, *J* = 3.0 Hz, 0.5H, 3), 6.00 (d, *J* = 3.0 Hz, 0.5H, 3), 4.38 (m, 1H, 18), 4.28 – 4.19 (m, 7H, 27), 4.11 (m, 1H, 27), 3.92 – 3.72 (m, 5H, 11, 13, 16), 3.16 – 2.62 (m, 25H, 30, 19, 9, 3', 4', 4, 6, 5), 1.81 – 1.35 (m, 32H, 28, 29).

2-(4-(((2-amino-4-oxo-3,4-dihydropteridin-6-yl)methyl)amino)benzamido)-5-((2-mercaptoethyl)amino)-5-oxopentanoic acid*TFA (5):

0.393 g (173 µmol, loading: 0.44 mmol/g) of a 4-methoxytrityl resin preloaded with 2-aminoethanethiol were swollen in 8 mL dichloromethane (DCM) for 30 minutes. After the solvent was removed, a solution of 382 mg (857 µmol, 99 %) folic acid and 450 mg (865 µmol, 95 %) PyBOP dissolved in 10 mL DMSO is added. Afterwards 412 µL (2.41 mmol, 99.5 %) diisopropylethylamine (DIPEA) is added dropwise. The reaction was shaken over night at 40 °C in the oven. After removal of the solvent, the resin was washed with DMSO, DMF, DCM and methanol (5x10 mL each). A negative Ninhydrin test of the resulting resin proved no primary amine being present anymore. For cleaving the product from the resin, 8 mL TFA/DCM (v:v 1:1) is added. The mixture is shaken for 1 h at room temperature. The removed orange solution is poured into 400 mL diethylether to precipitate the product. 62.3 mg of an orange solid are obtained with a yield of 53 % (62.3 mg). ESI-ToF-MS: m/z 501.16 $[M+H]^+$.

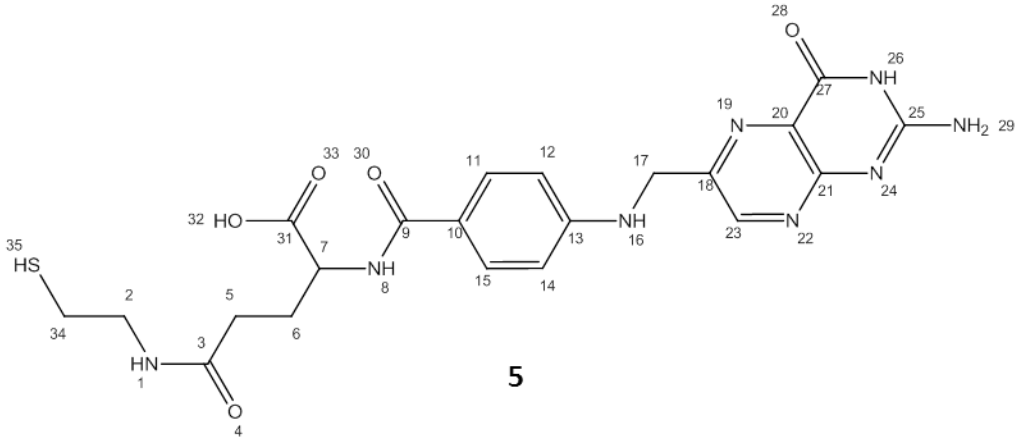

5

^{1}H-NMR (300 MHz, DMSO-d_6) δ 8.68 (d, J = 1.0 Hz, 1H, 23 (long range with 17 assigned by 2D measurement), 8.11 – 7.88 (m, 2H, 1, 8), 7.66 (dd, J = 9.0, 3.0 Hz, 2H, 11/15), 7.44 (broad, 3H, 26, 29), 6.62 (dd, J = 9.0, 1.0 Hz, 2H, 12/14), 4.52 (s, 2H, 17, coupling to 23 assigned by 2D measurement), 4.38 – 4.23 (m, 1H, 7), 3.59 – 3.50 (m, 1H, 16), 3.28 – 3.08 (m, 2H, 2), 2.45 – 1.76 (m, 6H, 5, 6, 34). Furthermore the molecular formula is proven by high-resolution MS: formula: $C_{21}H_{25}N_8O_5S$.

2-(4-(((2-amino-4-oxo-3,4-dihydropteridin-6-yl)methyl)amino)benzamido)-5-((2-((3-(2-(2-amino-7-(furan-2-yl)-7,8-dihydroquinazolin-5(6H)-ylidene)hydrazinyl)-3-oxopropyl)disulfanyl)ethyl)amino)-5-oxopentanoic acid (6):

26.4 mg **3** (52.7 µmol, 88 %) were dissolved in 1 mL DMSO. 27 mg **5** (39.6 µmol, 90 %) were dissolved in 2 mL DMSO separately and added dropwise to the solution of **3** within 2 minutes. The yellow reaction mixture was stirred at room temperature for 1 day. Precipitation of the product in 50 µL diethylether resulted in an orange powder with a yield of 22 % (12.0 mg) and a purity of 60 %. The product was not further purified. ESI-ToF-MS: m/z 830 $[M+H]^+$. Isomeric ratio: 0.4/0.6:

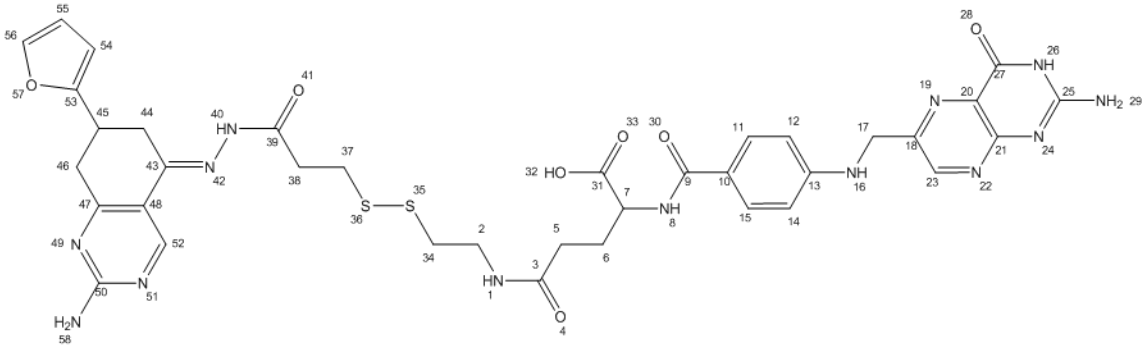

6

^{1}H-NMR (300 MHz, DMSO-d_6) δ 11.36 (d, *J* = 34.1 Hz, 1H, 32), 10.58 (s, 0.6H, 40)*, 10.43 (s, 0.4, 40), 8.75 (s, 0.6H, 52)*, 8.57 (s,0.4H, 52), 8.64 (s, 1H, 23), 8.01 (m, 2H, 2 NH, 1, 8), 7.79 (s, 1H, 26), 7.70 – 7.57 (m, 3H, 11, 15, 56), 6.98 (broad, 4H,29, 58), 6.64 (d, *J* = 9.0 Hz, 2H, 12, 14), 6.38 (m 1H 55), 6.16 (m, 1H, 56 ArH), 4.48 (d, J = 5.0 Hz, 2H, 17), 4.32 (m, 1H, 7), 3.56 (d, *J* =5.0 Hz, 1H, 16), 2.90 – 1.77 (m, overlapping with solvent, 2, 5, 6, 34, 37, 38, 44, 46, 45).

8 References

1. Bundesamt, D.S. *Todesursache 2011: Krebs immer häufiger*. 2013 [cited 2013 May 10th]; Available from: https://www.destatis.de/DE/ZahlenFakten/GesellschaftStaat/Gesundheit/Todesursachen/Aktuell.html.

2. *Die häufigsten Krebsarten in Deutschland 2006*. [cited 2013 July 4th]; Available from: http://www.roche.de/pharma/indikation/onkologie/darmkrebs/images/1000_1_1_Pat.jpg.

3. *Krebs in Deutschland*. [cited 2013 July 3rd]; Available from: http://www.krebsdaten.de/Krebs/DE/Content/Publikationen/Krebs_in_Deutschland/kid_2012/kid_2012_c43.pdf?__blob=publicationFile.

4. *Hautkrebs*. [cited 2013 July 4th]; Available from: http://www.hautkrebs.de.

5. Damsky, W.E., N. Theodosakis, and M. Bosenberg, *Melanoma metastasis: new concepts and evolving paradigms.* Oncogene, online publication 3 June 2013: p. Ahead of Print.

6. Kimpfler, S., et al., *Skin Melanoma Development in ret Transgenic Mice Despite the Depletion of CD25+Foxp3+ Regulatory T Cells in Lymphoid Organs.* J. Immunol., 2009. **183**(10): p. 6330-6337.

7. Dillman, R.O., *Cancer immunotherapy.* Cancer Biother. Radiopharm., 2011. **26**(1): p. 1-64.

8. Bopp, T., et al., *New strategies for the manipulation of adaptive immune responses.* Cancer Immunol. Immunother., 2010. **59**(9): p. 1443-1448.

9. Scott, A.M., J.D. Wolchok, and L.J. Old, *Antibody therapy of cancer.* Nat. Rev. Cancer, 2012. **12**(4): p. 278-287.

10. Ducry, L. and B. Stump, *Antibody-Drug Conjugates: Linking Cytotoxic Payloads to Monoclonal Antibodies.* Bioconjugate Chem., 2010. **21**(1): p. 5-13.

11. Sakaguchi, S., et al., *Regulatory T cells: how do they suppress immune responses?* Int. Immunol., 2009. **21**(10): p. 1105-1111.

12. Bopp, T., et al., *Cyclic adenosine monophosphate is a key component of regulatory T cell-mediated suppression.* J Exp Med, 2007. **204**(6): p. 1303-10.

13. Bopp, T., et al., *Inhibition of cAMP Degradation Improves Regulatory T Cell-Mediated Suppression.* J. Immunol., 2009. **182**(7): p. 4017-4024.

14. Sudimack, J. and R.J. Lee, *Targeted drug delivery via the folate receptor.* Adv. Drug Delivery Rev., 2000. **41**(2): p. 147-162.

15. Trail, P.A., H.D. King, and G.M. Dubowchik, *Monoclonal antibody drug immunoconjugates for targeted treatment of cancer.* Cancer Immunol. Immunother., 2003. **52**(5): p. 328-337.

16. Wang, S. and P.S. Low, *Folate-mediated targeting of antineoplastic drugs, imaging agents, and nucleic acids to cancer cells.* J. Controlled Release, 1998. **53**(1-3): p. 39-48.

17. Garcia-Bennett, A., M. Nees, and B. Fadeel, *In search of the Holy Grail: Folate-targeted nanoparticles for cancer therapy.* Biochem. Pharmacol., 2011. **81**(8): p. 976-984.

18. Siegel, R., D. Naishadham, and A. Jemal, *Cancer statistics, 2012.* CA Cancer J Clin, 2012. **62**(1): p. 10-29.

19. Siegel, R., et al., *Cancer statistics, 2011: the impact of eliminating socioeconomic and racial disparities on premature cancer deaths.* CA Cancer J Clin, 2011. **61**(4): p. 212-36.

20. Siegel, R., et al., *Cancer treatment and survivorship statistics, 2012.* CA Cancer J Clin, 2012. **62**(4): p. 220-41.

21. Moll, I., *Dermatologie*. 6 ed, ed. A.u.K. Bob. 2005: Thieme Verlag.

22. Eggermont, A.M.M. and C. Robert, *New drugs in melanoma: it's a whole new world.* Eur J Cancer, 2011. **47**(14): p. 2150-7.

23. Sanada, M., et al., *Killing and mutagenic actions of dacarbazine, a chemotherapeutic alkylating agent, on human and mouse cells: effects of Mgmt and Mlh1 mutations.* DNA Repair, 2004. **3**(4): p. 413-420.

24. Lui, P., et al., *Treatments for metastatic melanoma: synthesis of evidence from randomized trials.* Cancer Treat Rev, 2007. **33**(8): p. 665-80.

25. Pretto, F. and D. Neri, *Pharmacotherapy of metastatic melanoma: Emerging trends and opportunities for a cure.* Pharmacol. Ther.: p. Ahead of Print.

26. Aplin, A.E., F.M. Kaplan, and Y. Shao, *Mechanisms of Resistance to RAF Inhibitors in Melanoma.* J. Invest. Dermatol., 2011. **131**(9): p. 1817-1820.

27. Hodi, F.S., et al., *Improved survival with ipilimumab in patients with metastatic melanoma.* N. Engl. J. Med., 2010. **363**(8): p. 711-723.

28. Tarhini, A.A., *Tremelimumab: a review of development to date in solid tumors.* Immunotherapy, 2013. **5**(3): p. 215-229.

29. H.P.Rang, M.M.D., J.M.Ritter, R.J.Flower, G.Henderson, *Rang and Dale's Pharmacology*. 7 ed. 2012: Elsevier.

30. Villanueva, J. and M. Herlyn, *Melanoma and the tumor microenvironment.* Curr. Oncol. Rep., 2008. **10**(5): p. 439-446.

31. Defer, N., M. Best-Belpomme, and J. Hanoune, *Tissue specificity and physiological relevance of various isoforms of adenylyl cyclase.* Am. J. Physiol., 2000. **279**(3, Pt. 2): p. F400-F416.

32. Seifert, R., et al., *Inhibitors of membranous adenylyl cyclases.* Trends Pharmacol. Sci., 2012. **33**(2): p. 64-78.

33. *cAMP pathway*. [cited 2013 July 17th]; Available from: http://bio1151.nicerweb.com/Locked/media/ch11/11_10cAMPSecondMessenger_L.jpg.

34. Kenneth Murphy, P.T., Mark Walport, *Janeway's Immuno biology*. 7 ed. 2008, New York: Garland Science, Tayylor & Francis Group, LLC.

35. Bodor, J., et al., *Suppression of T-cell responsiveness by inducible cAMP early repressor (ICER).* Journal of Leukocyte Biology, 2001. **69**(6): p. 1053-1059.

36. Bodor, J., et al., *Cyclic AMP underpins suppression by regulatory T cells.* Eur. J. Immunol., 2012. **42**(6): p. 1375-1384.

37. Onda, T., et al., *Type-specific regulation of adenylyl cyclase. Selective pharmacological stimulation and inhibition of adenylyl cyclase isoforms.* J. Biol. Chem., 2001. **276**(51): p. 47785-47793.

38. Johnson, R.A. and I. Shoshani, *Kinetics of "P"-site-mediated inhibition of adenylyl cyclase and the requirements for substrate.* J. Biol. Chem., 1990. **265**(20): p. 11595-600.

39. Seifert, R., et al., *Inhibitors of membranous adenylyl cyclases.* Trends Pharmacol Sci, 2012. **33**(2): p. 64-78.

40. Iwatsubo, K., et al., *Direct inhibition of type 5 adenylyl cyclase prevents myocardial apoptosis without functional deterioration.* J Biol Chem, 2004. **279**(39): p. 40938-45.

41. Watkins, C.L., et al., *Cellular uptake, distribution and cytotoxicity of the hydrophobic cell penetrating peptide sequence PFVYLI linked to the proapoptotic domain peptide PAD.* J. Controlled Release, 2009. **140**(3): p. 237-244.

42. Frankel, A.D. and C.O. Pabo, *Cellular uptake of the tat protein from human immunodeficiency virus.* Cell (Cambridge, Mass.), 1988. **55**(6): p. 1189-93.

43. Eguchi, A. and S.F. Dowdy, *siRNA delivery using peptide transduction domains.* Trends Pharmacol. Sci., 2009. **30**(7): p. 341-345.

44. Maee, M. and U. Langel, *Cell-penetrating peptides as vectors for peptide, protein and oligonucleotide delivery.* Curr. Opin. Pharmacol., 2006. **6**(5): p. 509-514.

45. Jones, A.T. and E.J. Sayers, *Cell entry of cell penetrating peptides: tales of tails wagging dogs.* J Control Release, 2012. **161**(2): p. 582-91.

46. Dietz, G.P.H. and M. Bδhr, *Delivery of bioactive molecules into the cell: the Trojan horse approach.* Molecular and Cellular Neuroscience, 2004. **27**(2): p. 85-131.

47. Milletti, F., *Cell-penetrating peptides: classes, origin, and current landscape.* Drug Discov Today, 2012. **17**(15-16): p. 850-60.

48. Heitz, F., M.C. Morris, and G. Divita, *Twenty years of cell-penetrating peptides: from molecular mechanisms to therapeutics.* Br. J. Pharmacol., 2009. **157**(2): p. 195-206.

49. Richard, J.P., et al., *Cellular uptake of unconjugated TAT peptide involves clathrin-dependent endocytosis and heparan sulfate receptors.* J. Biol. Chem., 2005. **280**(15): p. 15300-15306.

50. Fittipaldi, A., et al., *Cell Membrane Lipid Rafts Mediate Caveolar Endocytosis of HIV-1 Tat Fusion Proteins.* J. Biol. Chem., 2003. **278**(36): p. 34141-34149.

51. Wadia, J.S., R.V. Stan, and S.F. Dowdy, *Transducible TAT-HA fusogenic peptide enhances escape of TAT-fusion proteins after lipid raft macropinocytosis.* Nat. Med. (N. Y., NY, U. S.), 2004. **10**(3): p. 310-315.

52. Thundimadathil, J., *Drug delivery using cell-penetrating peptides. Advances in the design and application of cell-penetrating peptides has demonstrated their potential in molecular medicine.* Drug Discovery Dev., 2013. **16**(1): p. 22-23.

53. Fischer, R., et al., *Break on through to the other side-biophysics and cell biology shed light on cell-penetrating peptides.* ChemBioChem, 2005. **6**(12): p. 2126-2142.

54. Stewart, K.M., K.L. Horton, and S.O. Kelley, *Cell-penetrating peptides as delivery vehicles for biology and medicine.* Org. Biomol. Chem., 2008. **6**(13): p. 2242-2255.

55. Thomas D. Pollard, W.C.E., *Cell Biology*. Vol. 2. 2008, Berlin, Heidelberg: Springer.

56. Swanson, J.A. and C. Watts, *Macropinocytosis.* Trends Cell Biol, 1995. **5**(11): p. 424-8.

57. Parton, R.G. and A.A. Richards, *Lipid rafts and caveolae as portals for endocytosis: New insights and common mechanisms.* Traffic (Oxford, U. K.), 2003. **4**(11): p. 724-738.

58. Trabulo, S., et al., *Cell-penetrating peptides - mechanisms of cellular uptake and generation of delivery systems.* Pharmaceuticals, 2010. **3**: p. 961-993.

59. Lundin, P., et al., *Distinct Uptake Routes of Cell-Penetrating Peptide Conjugates.* Bioconjugate Chem., 2008. **19**(12): p. 2535-2542.

60. Maitani, Y. and Y. Hattori, *Oligoarginine-PEG-lipid particles for gene delivery.* Expert Opin. Drug Delivery, 2009. **6**(10): p. 1065-1077.

61. Kalia, J. and R.T. Raines, *Hydrolytic stability of hydrazones and oximes.* Angew Chem Int Ed Engl, 2008. **47**(39): p. 7523-6.

62. Kaneko, T., et al., *New hydrazone derivatives of Adriamycin and their immunoconjugates - a correlation between acid stability and cytotoxicity.* Bioconjugate Chem., 1991. **2**(3): p. 133-41.

63. Beat Ernst, A.V., *Moderne Pharmakokinetik*. 2010, Weihnheim: WILEY-VCH.

64. Mueller, C. and R. Schibli, *Folic acid conjugates for nuclear imaging of folate receptor-positive cancer.* J. Nucl. Med., 2011. **52**(1): p. 1-4.

65. Ansell, S.M., P.G. Tardi, and S.S. Buchkowsky, *3-(2-pyridyldithio)propionic acid hydrazide as a cross-linker in the formation of liposome-antibody conjugates.* Bioconjug Chem, 1996. **7**(4): p. 490-6.

66. Zara, J.J., et al., *A carbohydrate-directed heterobifunctional cross-linking reagent for the synthesis of immunoconjugates.* Anal. Biochem., 1991. **194**(1): p. 156-62.

67. Banerjee, S. and R. Goswami, *GST profile expression study in some selected plants: in silico approach.* Mol. Cell. Biochem., 2013. **380**(1-2): p. 283-300.

68. Aubry, S., et al., *Cell-surface thiols affect cell entry of disulfide-conjugated peptides.* FASEB J., 2009. **23**(9): p. 2956-2967, 10.1096/fj.08-127563.

69. von, D.M., et al., *Synthesis and solid state structure of a hydrazone-disulfide macrocycle and its dynamic covalent ring-opening under acidic and basic conditions.* Org. Biomol. Chem., 2010. **8**(20): p. 4617-4624.

70. van, d.V.A.J., et al., *Synthesis of Pyridyl Disulfide-Functionalized Nanoparticles for Conjugating Thiol-Containing Small Molecules, Peptides, and Proteins.* Bioconjugate Chem., 2010. **21**(4): p. 653-662.

71. *Spectral Database for Organix Compounds SDBS*. [cited 2013 July 10th]; Available from: adbs.riodb.aist.go.jp.

72. C.E.Castello. *The Association of Biomolecular Resource Facilities*. 30 July 1995 [cited 2013 July 17th]; Available from: http://www.abrf.org/ABRFNews/1994/April1994/apr94maldi.html.

73. Atkinson, S.F., et al., *Conjugation of folate via gelonin carbohydrate residues retains ribosomal-inactivating properties of the toxin and permits targeting to folate receptor positive cells.* J. Biol. Chem., 2001. **276**(30): p. 27930-27935.

74. Zhang, C., et al., *Targeted minicircle DNA delivery using folate-poly(ethylene glycol)-polyethylenimine as non-viral carrier.* Biomaterials, 2010. **31**(23): p. 6075-86.

75. Pasut, G., et al., *Antitumoral activity of PEG-gemcitabine prodrugs targeted by folic acid.* J. Controlled Release, 2008. **127**(3): p. 239-248.

76. Pinhassi, R.I., et al., *Arabinogalactan-Folic Acid-Drug Conjugate for Targeted Delivery and Target-Activated Release of Anticancer Drugs to Folate Receptor-Overexpressing Cells.* Biomacromolecules, 2010. **11**(1): p. 294-303.

Affirmation in lieu of an oath

I hereby affirm that the thesis entitled: Synthesis of modifications of an adenylyl cyclase inhibitor conjugated with a peptide and folic acid for the application in tumor immunotherapy is my own work, written independently and without assistance other than the resources cited.

I have indicated the bodies of work, including tables and illustrations, which originate from earlier work of other authors. In each case I have quoted the origin thereof.

This thesis has not been submitted, in either identical or similar form, to any other examination authority or university, and has not yet been published.

Mainz, 25th July 2013

Lisa-Maria Ackermann